Journal Pre-proof

Comprehensive *in vitro* and *in silico* analysis of *Piliostigma thonningii's* bioactive compounds as multifunctional inhibitors of α-amylase, α-glucosidase, and oxidative stress for enhanced glycemic regulation

Alfred Sisinvou, Honoré Wangso, Hamadou Mamoudou, Sali Mouhamadou, Benoît Bargui Koubala, Mohamed F AlAjmi, Celine Henoumont, Sophie Laurent, Mohit Agrawal, Emmanuel Talla

PII: S2950-1946(25)00393-0

DOI: https://doi.org/10.1016/j.microb.2025.100625

Reference: MICROB100625

To appear in: *The Microbe*

Received date: 17 March 2025
Revised date: 5 September 2025
Accepted date: 20 November 2025

Please cite this article as: Alfred Sisinvou, Honoré Wangso, Hamadou Mamoudou, Sali Mouhamadou, Benoît Bargui Koubala, Mohamed F AlAjmi, Celine Henoumont, Sophie Laurent, Mohit Agrawal and Emmanuel Talla, Comprehensive *in vitro* and *in silico* analysis of *Piliostigma thonningii's* bioactive compounds as multifunctional inhibitors of α-amylase, α-glucosidase, and oxidative stress for enhanced glycemic regulation, *The Microbe,* (2025) doi:https://doi.org/10.1016/j.microb.2025.100625

the journal pertain.

Comprehensive *in vitro* and *in silico* analysis of *Piliostigma thonningii's* bioactive compounds as multifunctional inhibitors of α-amylase, α-glucosidase, and oxidative stress for enhanced glycemic regulation

Alfred Sisinvou[a], Honoré Wangso[a,c*], Hamadou Mamoudou[b], Sali Mouhamadou[a,c], Benoît Bargui Koubala[a,*], Prof. Mohamed F AlAjmi[d], Celine Henoumont[e], Sophie Laurent[e], Mohit Agrawal[f], Emmanuel Talla[g]

[a]Department of Chemistry, Faculty of Science, University of Maroua, Maroua P.O. Box 814, Cameroon
[b]Department of Biological Sciences, Biochemistry, Bioinformatics, and Bioactive Compounds for Health Promotion, Research Unit, Faculty of Science, University of Maroua, P. O. Box 814, Maroua, Cameroon
[c]Department of Chemistry, Faculty of Science, University of Garoua, Garoua P.O. Box 346, Cameroon
[d]Department of Pharmacognosy, College of Pharmacy, King Saud University, P.O Box 2457, Riyadh 11451, Saudi Arabia
[e]Department of General, Organic Chemistry and Biomedical, Laboratory of NMR and molecular Imaging, university of MONS, Belgium
[f]School of Medical & Allied Sciences, K.R. Mangalam University, Gurugram, Haryana, India.
[g]Department of Chemistry, Faculty of Science, University of Ngaoundere, P.O. Box 445 Ngaoundere, Cameroon

*Corresponding authors mail: bkoubala@yahoo.fr (BBK); honorewangso@gmail.com (HW)

Abstract

Type 2 diabetes mellitus is a growing global health crisis requiring effective management strategies, including the control of postprandial hyperglycemia. Inhibiting key carbohydrate-digesting enzymes, namely α-amylase and α-glucosidase, is a proven therapeutic approach. However, many current inhibitors have undesirable side effects. This study examines the anti-diabetic and antioxidant potential of bioactive compounds isolated from *Piliostigma thonningii*, a plant with a history of traditional use in treating diabetes, employing both *in vitro* and *in silico* approaches. A multifaceted approach was employed to elucidate the chemical profile and bioactive potential of the *P. thonningii* methanolic extract. This approach combined chromatographic separation, spectroscopic characterization, and *in vitro* antioxidant (DPPH, ABTS, HRSA, and FRAP assays) and anti-diabetic evaluations. Molecular docking and dynamics simulations were employed to predict the binding affinities and stabilities of isolated compounds with α-amylase and α-glucosidase. The methanolic extract exhibited notable antioxidant activity, comparable to that of the synthetic antioxidant BHT. The highest DPPH anti-radical activity was exhibited by kaempferol 3-O-α-L-rhamnopyranosyl-(1-2)-β-D-galactopyranoside (**10**) (IC_{50} = 172.45 µg/mL, 69.48% inhibition). In addition, the methanol (MeOH) extract demonstrated potent anti-diabetic activity *in vitro*, exhibiting the lowest IC_{50}

values for both α-amylase (184.45 µg/mL) and α-glucosidase (175.61 µg/mL) inhibition. Among the isolated compounds, genkwanin (**5**) displayed promising inhibitory activity against both enzymes (α-amylase IC_{50}: 180.95 µg/mL, α-glucosidase IC_{50}: 174.95 µg/mL), while epicatechin (**4**) and shikimic acid (**2**) showed notable and moderate α-glucosidase inhibitory activities, respectively (epicatechin IC_{50}: 201.51 µg/mL, shikimic acid IC_{50}: 196.25 µg/mL). Vitexin (**6**) and genkwanin (**5**) were identified as the most potent α-amylase and α-glucosidase inhibitors *in silico*, with binding affinities of -8.6 kcal/mol and -8.5 kcal/mol, respectively. This study identifies compounds derived from *P. thonningii*, particularly vitexin (**6**) and genkwanin (**5**), as promising natural inhibitors of α-amylase and α-glucosidase. The findings indicate that the plant may serve as a valuable source of antioxidants and anti-diabetic compounds, thereby supporting its traditional medicinal applications and suggesting a pathway for the development of new, natural-based therapies for type 2 diabetes.

Keywords:

Piliostigma thonningii, α-amylase inhibitors, α -glucosidase inhibitors, type 2 diabetes, molecular docking, molecular dynamics simulations

Abbreviations

ATBS	2,2-azino-bis (3-ethylbenzylthiozoline-6-sulphonic acid)
BHT	Butylated Hydroxytoluene
DPPH	2,2- diphenyl-1-picrylhydrazyl
FRAP	Ferric-reducing antioxidant power
HRSA	Hydroxyl Radical Scavenging Activity
LGA	Lamarck Genetic Algorithm
PDB	Protein Data Bank
RMSD	Root-Mean-Square Deviation
T2D/M	Type 2 Diabetes/ Mellitus

1. Introduction

Piliostigma thonningii, a plant in the *Piliostigma* genus, has gained attention in the field of ethnomedicine due to its therapeutic uses. This genus includes two species, *Piliostigma reticulatum* and *Piliostigma thonningii*, which are traditionally used in Africa and Asia to treat

various diseases including diabetes, infections, and inflammation (I. B. Abubakar et al., 2024; M. O. Afolayan et al., 2023; Hailemariam et al., 2021; Mouhamadou, Dalhatou, Dobe, et al., 2023; Mouhamadou, Dalhatou, Obada, et al., 2023). Both species belong to the Caesalpinioideae subfamily of the Fabaceae family and are perennial plants. *Piliostigma thonningii* is known for its variable petal colors, ranging from white to pink. While *P. reticulatum* and *P. thonningii* share some similarities in stigma shape, they differ in leaf structure, texture, and geographical distribution (I. B. Abubakar et al., 2024; Hailemariam et al., 2021; Mouhamadou, Dalhatou, Dobe, et al., 2023; Mouhamadou, Dalhatou, Obada, et al., 2023; Ogbiko et al., 2024). The botanical name 'thonningii' was chosen to honor the Danish botanist Peter Thonning, who originally described the species under the Bauhinia genus (Hamadou et al., 2020; Oscar Ditchou Nganso, Sidjui Sidjui, et al., 2020). This tree is found in tropical and subtropical regions, including Cameroon, Nigeria, Kenya, Senegal, Namibia, as well as India, China, and Cuba. It is known by different names in local communities, such as “Vessi” and “Barkee-hi” in northern Cameroon, “Camel’s Foot Tree” or “Monkey Bread” in English, and “Pied de Chameau” or “Semalier” in French (I. B. Abubakar et al., 2024; M. O. Afolayan et al., 2023; Hailemariam et al., 2021; Ogbiko et al., 2024). These various names highlight the cultural and medicinal significance of the plant in different regions.

The extensive utilization of *Piliostigma thonningii* in traditional medicine is predominantly attributed to the plant's diverse phytochemical composition. Preparations derived from the roots, bark, and leaves of the plant, including decoctions, infusions, and macerations, have been traditionally employed in the treatment of a range of health conditions. Such conditions include metabolic disorders such as diabetes, infectious diseases such as malaria and gonorrhea, as well as inflammatory conditions such as arthritis and ulcers (I. B. Abubakar et al., 2024; M. Afolayan et al., 2018; M. O. Afolayan et al., 2023; Hailemariam et al., 2021; Nurudeen et al., 2024; Ogbiko et al., 2024). In addition to its efficacy in treating chronic diseases, the plant has also demonstrated effectiveness in addressing acute conditions, including fever, gastric discomfort, and wound infections. The extensive medicinal potential of *Piliostigma thonningii* has prompted a number of pharmacological studies aimed at elucidating the bioactive compounds and their mechanisms of action.

Phytochemical analyses of the *Piliostigma* species, including *P. thonningii*, have identified a diverse range of secondary metabolites, including terpenoids, flavonoids, tannins, saponins, and alkaloids (M. O. Afolayan et al., 2023; Ogbiko et al., 2024). These compounds are known to

possess a range of pharmacological activities, including anti-inflammatory, antimicrobial, antioxidant, and antidiabetic effects (Amang à Ngnoung et al., 2023; Hamadou et al., 2022; Himeda et al., 2022; Luka et al., 2024; Nurudeen et al., 2024; Wangso et al., 2022). Specific bioactive compounds isolated from *P. thonningii* include D-3-O-methylchiroinositol, a molecule with reported antidiabetic, antioxidant, and antilipidemic activities. This compound has been particularly noted for its potential to modulate glucose metabolism, making it a promising candidate for managing type 2 diabetes (Ogbiko et al., 2024). Additionally, C-methylflavanols have been identified in this species, demonstrating significant anti-inflammatory and antibacterial properties (I. B. Abubakar et al., 2024; M. O. Afolayan et al., 2023).

In light of the rising incidence of metabolic disorders such as type 2 diabetes, the investigation of natural compounds that can regulate carbohydrate metabolism has emerged as a pivotal research area (Mueed et al., 2023; Nganso Ditchou et al., 2024; Núñez et al., 2023; Su et al., 2024; Tiwari et al., 2023). While previous studies have reported the traditional uses and general phytochemical composition of *Piliostigma thonningii*, a systematic investigation combining both *in vitro* and *in silico* methodologies to identify and characterize its specific anti-diabetic lead compounds has not been conducted. The diverse phytoconstituents present in *Piliostigma thonningii* offer a valuable source of novel bioactive compounds. The present study aims to examine the potential of these compounds as inhibitors of key enzymes involved in carbohydrate metabolism, namely α-amylase and α-glucosidase. Both enzymes are instrumental in the breakdown of starch and disaccharides into glucose, and their inhibition has been identified as an effective strategy for controlling postprandial blood glucose levels in diabetic patients.

In this context, *in vitro* and *in silico* methods provide effective tools for evaluating the inhibitory effects of *Piliostigma thonningii* extracts and isolated compounds on α-amylase and α-glucosidase activity. These techniques facilitate the identification of promising therapeutic agents and provide insights into their molecular mechanisms of action. By exploring the bioactive potential of *Piliostigma thonningii*, this study will contribute to the development of novel, plant-derived therapies for the management of type 2 diabetes.

2. Materials and Methods

The diagram (Fig. 1) presents a comprehensive methodology for the extraction, purification, characterization, and biological evaluation of bioactive compounds, with particular emphasis

on the importance of each step in understanding the therapeutic potential of plant-derived substances.

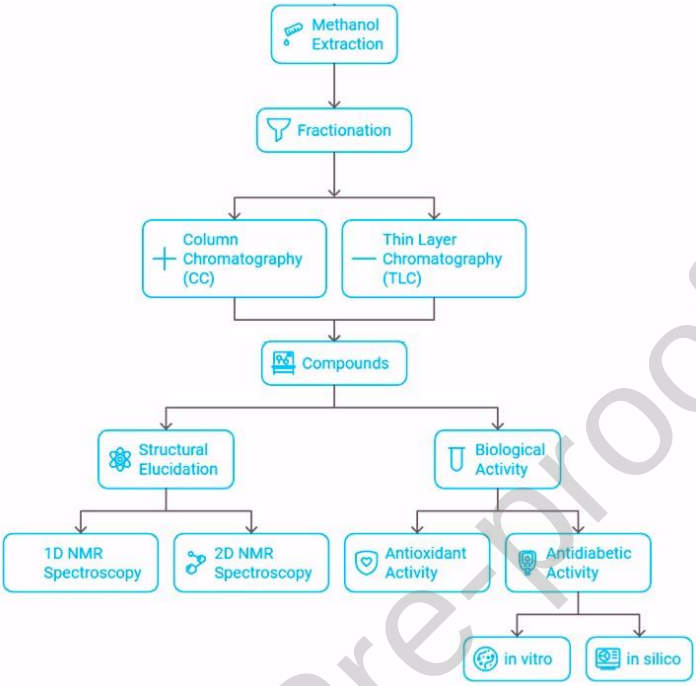

Fig. 1. General procedure

2.1. Plant material

The leaves of *Piliostigma thonningii* (Fig. 2) were harvested in Dagai, a village situated in the Ndoukoula Subdivision of Diamare, Far North Region, Cameroon, on October 25, 2021. The plant was identified at the Herbarium of the School of Fauna of Garoua, and a voucher specimen was deposited under the reference 1345/HEFG.

Fig. 2. *Piliostigma thonningii*

2.2. Chemicals

The following chemical reagents were obtained from Sigma-Aldrich Chemical Company (Mumbai, India): 2,6-di-tert-butyl-4-methylphenol (BHT), 2,2-diphenyl-1-picrylhydrazyl radical (DPPH), 6-hydroxy-2,5,7,8-tetramethylchromane-2-carboxylic acid (Trolox, 98%), 2,4,6-tris(2-pyridyl)-s-triazine (TPTZ, 98%), and 2,2'-azinobis (3-ethylbenzothiazoline-6-sulfonic acid) diammonium salt (ABTS, 98%).

Additional reagents were sourced from Sigma-Aldrich (St. Louis, MO, USA), including 3,5-dinitrosalicylic acid, α-amylase enzyme, α-glucosidase enzyme, acarbose, and p-nitrophenyl-α-D-glucopyranoside.

2.3. Bioactive compounds: extraction, isolation, and purification

2.3.1. Extraction of compounds from *P. thonningii*

The air-dried powdered leaves of *P. thonningii* (4 kg) were subjected to maceration in methanol (MeOH, 12 L) over three 72-hour periods. The resulting macerate was filtered and concentrated at room temperature, yielding 760.5 g of crude extract. A portion of the extract (356.3 g) was then partitioned using ethyl acetate (EtOAc) and water, resulting in two fractions: EtOAc (290.3 g) and aqueous (88 g) fractions.

2.3.2. Isolation and purification of compounds from *P. thonningii*

A subset of the EtOAc fraction (69.5 g) was separated via silica gel column chromatography using n-hexane, EtOAc, and MeOH solvent systems of increasing polarity. Fractions (500 mL each) were collected based on thin layer chromatography analysis and grouped into six sub-fractions (F-K). These sub-fractions were eluted using the following solvent ratios: F (20.2 g, n-hexane/EtOAc 1:0-4:1, v/v), G (13.4 g, n-hexane/EtOAc 3:1-1:1, v/v), H (8.4 g, n-hexane/EtOAc 9:11-1:3, v/v), I (21.4 g, n-hexane/EtOAc 1:4-1:19, v/v), J (9.3 g, EtOAc/MeOH 1:0-9:1, v/v), and K (6.6 g, n- EtOAc/MeOH 17:3-7:3, v/v). Successive column chromatography (CC) of sub-fractions F-K yielded the following compounds: **1** (35.2 mg, white powder, n-hexane/EtOAc 19:1, v/v), **2** (31.3 mg, white powder, n-hexane/EtOAc 4:1, v/v), **7** (40.8 mg, white powder, n-hexane/EtOAc 13:7, v/v), **3** (62.1 mg, n-hexane/EtOAc 2:3, v/v), **8** (18.1 mg, yellow crystalline solid, EtOAc/MeOH 19:1, v/v), **4** (19.3 mg, yellow crystalline solid, EtOAc/MeOH 9:1, v/v), **5** (16.3 mg, yellow solid, EtOAc/MeOH 17:3, v/v) and **6** (17.6 mg, white powder, EtOAc/MeOH 3:2, v/v).

A part of aqueous extract (57.4 g) was fractionated using an open CC, eluting with gradient systems of EtOAc/MeOH (1:0 to 0:1). A total 60 fractions (500 mL each) were collected to yield five combined sub-fractions (A1-A5) based on their thin layer chromatography profiles : A1 (7.8 g ; EtOAc/MeOH, 1:0-7:3, v/v), A2 (9.2 g ; EtOAc/MeOH, 17:3-2:3, v/v), A3 (10.2 g ; EtOAc/MeOH, 7:13-3:7, v/v), A4 (12.6 g ; EtOAc/MeOH, 1:3-3:17, v/v), A5 (11.3 g ; EtOAc/MeOH, 1:4-3:17, v/v). Successive column chromatography (CC) of sub-fractions A1-A5 yielded the following compounds: **9** (27.5 mg; yellow solid, EtOAc/MeOH, 3:7, v/v) and **10** (25.2 mg; yellow solid, EtOAc/MeOH, 3:7, v/v), an isocratic system. The three remaining sub-fractions contained complex mixtures that could not be resolved.

2.4. Spectroscopic data of *P. thonningii's* compounds

2H-chromen-2-one (1): ^{1}H NMR (600 MHz, $CDCl_3$) δ (ppm) 7.73 (d, J = 9.6 Hz, 1H), 7.54 (ddd, J = 8.5, 7.3, 1.6 Hz, 1H), 7.50 (dd, J = 7.7, 1.6 Hz, 1H), 7.35 (d, J = 8.3 Hz, 1H), 7.30 (td, J = 7.7, 1.6 Hz, 1H), 6.44 (d, J = 9.6 Hz, 1H) (Fig. S1). ^{13}C NMR (151 MHz, $CDCl_3$) δ (ppm) (ordered C2 – C10) 160.8, 116.9, 143.5, 127.8, 124.5, 131.8, 116.7, 118.8, 154.1 (Fig. S2).

Shikimic acid (2): ^{1}H NMR (500 MHz, Methanol-*d4*) δ (ppm) 6.84 (d, J = 3.7 Hz, 1H), 4.40 (t, J = 4.1 Hz, 1H), 4.04 (m, 1H), 3.70 (dd, J = 7.6, 4.2 Hz, 1H), 2.73 (dd, J = 18.3, 5.0 Hz, 1H), 2.22 (dd, J = 18.2, 5.8 Hz, 1H) (Fig. S4). ^{13}C NMR (126 MHz, Methanol-*d4*) δ (ppm) (ordered C1-C7) 131.1, 138.6, 67.4, 72.9, 68.5, 31.9, 170.3 (Fig. S5).

***n-eicosyl trans ferrulate (3)*:** ^{1}H NMR (600 MHz, $CDCl_3$) δ (ppm) 7.64 (d, J = 15.9 Hz, 1H), 7.10 (d, J = 8.1 Hz, 1H), 7.06 (s, 1H), 6.94 (d, J = 8.1 Hz, 1H), 6.32 (d, J = 15.9 Hz, 1H), 5.88 (s, 1H), 4.21 (t, J = 6.8 Hz, 2H), 3.95 (s, 3H), 1.72 (m, 2H), 1.42 (m, 2H), 1.37 (m, 2H), 1.32 (m, 2H), 1.30-1.24 (m, 28H), 0.91 (t, J = 7.0 Hz, 3H) (Fig. S7). ^{13}C NMR (151 MHz, $CDCl_3$) δ (ppm) (ordered C1-C30) 127.1, 109.3, 146.8, 147.9, 114.5, 123.1, 144.6, 115.7, 167.4, 55.9, 64.7, 28.8, 26.0, 29.3-29.7, 31.9, 22.7, 14.1 (Fig. S8).

Epicatechin (4): ^{1}H NMR (500 MHz, Methanol-*d4*) δ (ppm) 6.97 (m, 1H), 6.84 (dd, J = 8.2, 2.1 Hz, 1H), 6.72 (d, J = 8.2 Hz, 1H), 5.99 (d, J = 2.0 Hz, 1H), 5.95 (d, J = 2.0 Hz, 1H), 5.55 (dt, J = 4.2, 2.1 Hz, 1H), 5.06 (s, 1H), 3.02 (dd, J = 17.4, 4.7 Hz, 1H), 2.88 (dd, J = 17.4, 2.6 Hz, 1H) (Fig. S10). ^{13}C NMR (126 MHz, Methanol-*d4*) δ (ppm) (ordered C2-C16) 78.7, 70.0, 26.9, 99.4, 157.3, 96.6, 167.6, 95.9, 157.9, 131.5, 115.2, 146.4, 145.9, 116.0, 119.4 (Fig. S11).

Genkwanin (5): ^{1}H NMR (500 MHz, DMSO-*d6*) δ (ppm) 7.97 (d, J = 8.7 Hz, 2H), 6.94 (d, J = 8.7 Hz, 2H), 6.85 (s, 1H), 6.78 (d, J = 2.3 Hz, 1H), 6.38 (d, J = 2.3 Hz, 1H). 3.88 (s, 3H) (Fig. S13). ^{13}C NMR (151 MHz, DMSO-*d6*) δ (ppm) (ordered C2-C16) 164.6, 103.5, 182.4, 161.7, 98.4, 165.6, 93.1, 105.1, 157.7, 121.5, 129.0, 116.4, 161.8, 129.0, 116.4, 56.5 (Fig. S14).

Vitexin (6): ESI-MS $[M+Na]^{+}$ m/z 455.10 ($C_{21}H_{20}O_{10}$). Spectre IR νmax (cm^{-1}) : 2966, 2663, 1676, 1501, 1260. ^{1}H NMR (500 MHz, DMSO-*d6*) δ (ppm) 13.16 (s, 1H), 7.98 (d, J = 9.7 Hz, 2H), 6.84 (d, J = 9.7 Hz, 2H), 6.77 (s, 1H), 6.22 (s, 1H), 4.98-4.59 (d, J = 9.7 Hz, 1H), 3.80 (t, J = 9.2 Hz, 1H), 3.78 (m, 1H), 3.76 (t, J = 11.3 Hz, 1H), 3.73 (m, 1H), 3.70 (m, 2H) (Fig. S16). ^{13}C NMR (125 MHz, DMSO-*d6*) δ (ppm) (ordered C2-C21) 161.7, 102.9, 182.6, 105.1, 161.5, 98.4, 161.5, 104.5, 156.5, 122.1, 129.5, 116.3, 164.4, 129.5, 116.3, 73.8, 71.3, 79.1, 70.9, 82.2, 61.7 (Fig. S17).

Methyl β-D-glucopyranoside (7): ^{1}H NMR (500 MHz, Methanol-*d4*) δ (ppm) 4.73 (d, J = 3.7 Hz, 1H), 3.91 (dd, J = 3.4, 1.2 Hz, 1H), 3.84 – 3.76 (m, 1H), 3.79-3.68 (m, 2H), 3.43 (s, 3H) (Fig. S18). ^{13}C NMR (126 MHz, Methanol-*d4*) δ (ppm) (ordered C1-C7) 101.5, 72.3, 71.5, 71.1, 70.3, 62.8, 55.7 (Fig. S19).

3,3',4',5-tetrahydroxystilbene (8): ^{1}H NMR (500 MHz, Methanol-*d4*) δ (ppm) 7.01 (d, J = 2.0 Hz, 1H), 6.93 (d, J = 16 Hz, 1H), 6.85 (dd, J = 2.9 Hz, 1H), 6.78 (d, J= 16 Hz, 1H), 6.76 (d, J = 8.5 Hz, 1H), 6.47 (d, J = 2.0 Hz, 2H), 6.20 (t, J = 2.2 Hz, 1H) (Fig. S21). ^{13}C NMR (126 MHz, Methanol-*d4*) δ (ppm) (ordered C1-C14) 141.3, 106.2, 159.9, 102.7, 159.6, 106.7, 127.0, 129.7, 131.1, 113.9, 146.6, 146.5, 116.5, 120.2, (Fig. S22).

Isorhamnetin 3-O-rutinoside (9): ^{1}H NMR (600 MHz, DMSO-*d6*) δ (ppm) 7.99 (d, J = 8.4, 2.1 Hz, 1H), 7.86 (d, J = 2.1 HZ, 1H), 6.93 (d, J = 8.6 Hz, 1H), 6.43 (m, 1H), 6.21 (m, 1H), 5.32 (d, J = 7.6 Hz, 1H), 4.43 (m, 1H), 3.84 (s, 3H), 3.71-3.06 (m, 9H), 0.98 (dd, J = 6.2, 3.8 Hz, 3H) (Fig. S24). ^{13}C NMR (151 MHz, DMSO-*d6*) δ (ppm) (ordered C2-C28) 157.1, 133.6, 177.9, 161.7, 99.2, 164.6, 94.2, 160.4, 104.5, 121.4, 113.7, 147.5, 149.9, 115.6, 122.7, 56.1, 101.6, 74.7, 76.4, 70.8, 76.9, 67.4, 101.2, 71.1, 71.6, 72.3, 68.8, 18.2(Fig. S25).

Kaempferol 3-O-α-L-Rhamnopyranosyl (1-2)-β-D-galactopyranoside (10): ^{1}H NMR (500 MHz, Methanol-*d4*) δ (ppm) 8.04 (d, J = 9.6 Hz, 2H), 6.93 (d, J = 9.6 Hz, 2H), 6.79 (m, 1H), 6.45 (m, 1H),5.59 (m, 1H), 5.40 (d, J = 7.3 Hz, 1H), 3.89 – 3.26 (m, 9H), 1.29 (m, 3H) (Fig. S27). ^{13}C NMR (126 MHz, Methanol-*d4*) δ (ppm) (ordered C2-C27) 159.8, 135.4, 179.9, 162.9,

100.6, 163.6, 95.6, 158.1, 107.6, 122.8, 132.4, 116.2, 161.8, 132.4, 116.2, 103.7, 75.8, 78.5, 71.5, 78.1, 62.7, 99.9, 71.7, 72.1, 73.6, 71.3, 18.1(Fig. S28).

2.5. Crude extract and isolated compounds: *in vitro* assessment of antioxidant activities

2.5.1. Free radical scavenging activity DPPH

The antiradical activity of extracts and isolated compounds against the stable free radical 2,2-diphenyl-1-picrylhydrazyl (DPPH•) was assessed using a protocol modified from Sun et al. (2005). The DPPH• assay exploits the ability of antioxidants to scavenge free radicals, resulting in decolorization of the purple-colored solution, measurable as a decrease in optical density at 517 nm.

To conduct the assay, 150 µL of each sample (extract or isolated compound) was combined with 1500 µL of 1 mM DPPH• solution (in 70% ethanol) or butylated hydroxytoluene (BHT) standard solution at concentrations ranging from 0-250 µg/mL. The mixture was vortexed for 60 seconds and incubated in the dark at 35 ºC for 30 minutes. Subsequent measurements of optical density at 517 nm were performed using a spectrophotometer. Sample concentrations were calculated from a calibration curve generated using the BHT standard solution. The percentage of inhibition was calculated using the following equation:

$$\text{Inhibition (\%)} = \frac{(\text{O. D control} - \text{O. D test})}{\text{O. D control}} \times 100$$

where O.D test was the optical density of the sample and O.D control was the optical density of the standard solution.

2.5.2. Evaluation of the ABTS free radical scavenging activity

Assessment of 2,2-azino-bis (3-ethylbenzothiazoline-6-sulphonic acid) (ABTS) free radical scavenging activity was conducted according to the method outlined by Gao et al. (2019). The ABTS cation radical, characterized by its blue-green color, forms through the oxidation of the ammonium salt. This process involves the formation of an ABTS nitrogen atom in the presence of potassium persulfate. Upon addition of an antioxidant, the ABTS radical ($ABTS^{º+}$) undergoes reduction, trapping a proton ($H^º$) and resulting in decolorization. This reaction is quantifiable by measuring the absorbance at 745 nm.

To prepare the ABTS reagent, 50 mL of 7 mM $ABTS^{º+}$ was mixed with 50 mL of 2.45 mM potassium persulfate. For the assay, 1500 µL of diluted $ABTS^{º+}$ solution was combined with

500 µL of either standard solution (butylated hydroxytoluene, BHT) or sample (extracts or isolated compounds). Following a 5-minute agitation and 30-minute incubation in darkness, optical density was measured at 745 nm. Sample concentrations were subsequently determined using regression curves generated from BHT standards (0-250 µg/mL). The inhibition percentage was calculated as follows:

$$\text{Inhibition (\%)} = \frac{(\text{O. D control} - \text{O. D test})}{\text{O. D control}} \times 100$$

where O.D test was the optical density of the sample and O.D control was the optical density of the standard solution.

2.5.3. Ferric-reducing antioxidant power (FRAP)

The ferric reducing antioxidant power (FRAP) of the sample was determined using the protocol outlined by Benzie and Strain (1996). This assay exploits the antioxidant-mediated reduction of the Fe (III)-2,4,6-tris(2-pyridyl)-s-triazine (TPTZ) complex to its ferrous form, characterized by a blue coloration with maximum absorption at 593 nm. The intensity of this coloration is directly proportional to the antioxidant capacity of the tested sample.

To conduct the FRAP assay, 500 µL of sample extract, isolated compounds, or standard solution (butylated hydroxytoluene, BHT) was combined with 1500 µL of FRAP reagent, comprising 250 µL of 0.3 M acetate buffer (pH 3.6), 225 µL of 0.01 M TPTZ in 40 mM HCl, and 225 µL of 140 mM FeCl3. The mixture was vortexed for 5 minutes and incubated in the dark at room temperature (30°C) for 30 minutes. Subsequent measurement of optical density at 593 nm enabled sample concentration evaluation via calibration curves generated using ascorbic acid standards (0-250 µg/mL). The ferric-reducing antioxidant power was expressed as percentage inhibition according to the following formula:

$$\text{Inhibition (\%)} = \frac{(\text{O. D control} - \text{O. D test})}{\text{O. D control}} \times 100$$

where O.D test was the optical density of the sample and O.D control was the optical density of the standard solution.

2.5.4. Evaluation of hydroxyl radical scavenging activity (HRSA)

The hydroxyl radical scavenging activity (HRSA) of the samples was assessed using a modified version of the protocol described by Wangso et al. (2022). This assay is based on the Fenton

reaction; wherein ferrous sulfate reacts with hydrogen peroxide to generate hydroxyl radicals (•OH). The subsequent reaction between •OH and salicylic acid yields a pink-colored complex, which is detectable at 510 nm.

In the presence of antioxidants, the •OH-mediated color formation is inhibited, resulting in a decrease in absorbance. To conduct the HRSA assay, a reaction mixture was prepared by combining 0.5 mL of 9 mM $FeSO_4$, 0.5 mL of 0.03% H_2O_2, 0.5 mL of 9 mM salicylic acid in ethanol, and 1 mL of standard solution (butylated hydroxytoluene, BHT) or sample (extracts or isolated compounds). Following incubation at room temperature (35°C) in the dark for 40 minutes, the optical density was measured at 510 nm. Sample concentrations were quantified using calibration curves generated with BHT standards (0-250 µg/mL). The percentage of hydroxyl radical scavenging ability was calculated using the following equation:

$$\text{Inhibition (\%)} = \frac{(\text{O. D control} - \text{O. D test})}{\text{O. D control}} \times 100$$

Where O.D test was the optical density of the sample and O.D control was the optical density of the standard solution.

2.6. *In vitro* assessment of antidiabetic properties: inhibition of α-amylase and α-glucosidase

2.6.1. α -amylase inhibition assessment of crude extracts and isolated compounds

An *in vitro* assay was conducted to evaluate α-amylase inhibition, with methodology adapted from that outlined by Nganso Ditchou et al. (2024) and modified to some extent. This enzymatic reaction entails the hydrolysis of starch by pancreatic or salivary α-amylase, resulting in the production of reducing sugars that reduce 3,5-dinitrosalicylic acid to 3-amino-5-nitrosalicylic acid, which exhibits an absorbance at 540 nm. The presence of α-amylase inhibitors results in a reduction in enzymatic activity, which is reflected in a decrease in optical density at 540 nm.

In order to assess the inhibitory activity, 25 µL of the sample (extracts or isolated compounds) or acarbose (0-300 µg/mL) was combined with 25 µL of phosphate buffer (20 mM, pH 6.9) containing α-amylase (0.5 mg/mL). Subsequently, a 10-minute incubation period at 25°C was initiated, followed by the addition of 25 µL of a 0.5% starch solution in phosphate buffer (20 mM, pH 6.9). The reaction mixture was then incubated for an additional 10 minutes at 25°C. The reaction was terminated with 50 µL of 3,5-dinitrosalicylic acid color reagent, followed by

a 5-minute incubation period in a water bath and subsequent cooling to room temperature. Absorbance was then measured at 540 nm using a spectrophotometer. The percentage of inhibition was calculated according to the following formula:

$$\text{Inhibition (\%)} = \frac{(\text{O. D control} - \text{O. D test})}{\text{O. D control}} \times 100$$

where O.D test was the optical density of the sample and O.D control was the optical density of the standard solution.

2.6.2. α-glucosidase inhibition analysis of crude extracts and isolated compounds

An *in vitro* assay was conducted to evaluate α-glucosidase inhibition, with the methodology adapted from the protocol outlined by Nganso Ditchou et al. (2024). This enzymatic reaction involves the hydrolysis of p-nitrophenyl-α-D-glucopyranose, yielding p-nitrophenol, which was quantified spectrophotometrically at 400 nm.

In order to assess the inhibitory activity, 50 µL of the sample (extracts or isolated compounds) or acarbose (0-300 µg/mL) was combined with 100 µL of phosphate buffer (20 mM, pH 6.8) containing α-glucosidase (0.01 mg/mL) and pre-incubated at 25°C for 10 minutes. The reaction was initiated by the addition of 50 µL of a solution of p-nitrophenyl-α-D-glucopyranose at a concentration of 5 mM. Following a 15-minute incubation period at 37°C, 2 mL of 500 mM Na_2CO_3 was added to terminate the reaction. The optical density of the resulting yellow solution was then measured at 400 nm using a spectrophotometer. The percentage of inhibition was estimated as follows:

$$\text{Inhibition (\%)} = \frac{(\text{O.D control} - \text{O.D test})}{\text{O.D control}} \times 100$$

where $O.D_{test}$ was the optical density of the sample and $O.D_{control}$ was the optical density of the standard solution.

2.7. Computational approaches for antidiabetic assessment: molecular docking and molecular dynamics

2.7.1. Ligand preparation for docking study

The ligands employed in this study were compounds isolated and identified from *P. thonningii*. Two-dimensional (2D) structures of these compounds were constructed using ChemDraw Ultra (12.0) software and saved in SDF format. ChemDraw 3D was subsequently utilized to generate

three-dimensional (3D) structures, which were saved in PDB format. All generated 3D structures underwent energy minimization optimization using Chimera X V1.4 software. Lastly, the PDB format files of the ligands were prepared using AutoDock Vina software tools and exported in PDBQT format for subsequent molecular docking simulations.

2.7.2. Protein receptors preparation

The preparation of protein receptors is a crucial step in the process of studying their structure and function. The three-dimensional structures of human pancreatic α-amylase and human intestinal α-glucosidase were retrieved from the Protein Data Bank (PDB) (www.rcsb.org/pdb) using the PDB identifier 4GQR (Ibrahim et al., 2018; Nganso Ditchou et al., 2024) and 2QLY (Ibrahim et al., 2018; Nganso Ditchou et al., 2024), respectively. Subsequently, each structure was subjected to a process of elimination, whereby any water molecules and bound ligands were removed in order to isolate the protein receptor using AutoDock vina 1.5.7 tools. Then, polar hydrogen atoms were incorporated into the protein structure, and Kollman charges were assigned to all atoms. Finally, the prepared protein structure was energy minimized to obtain a relaxed conformation. This was typically achieved through the use of a force field-based approach within the selected molecular mechanics software. The resulting energy-minimized structure was then converted to the AutoDock Vina-compatible Protein Data Bank, Partial Charge (PDBQT) format, which was utilized for subsequent computational docking simulations.

2.7.3. Grid generation using AutoDock software for molecular docking

The molecular docking simulations were performed on α-glucosidase (PDB ID: 2QLY) and human pancreatic α-amylase (PDB ID: 4GQR). The grid dimensions for α-glucosidase were 47.4871, 32.7237, and 49.9909 Å (xyz points). For human pancreatic α-amylase, the grid dimensions were 34.6732, 35.2485, and 35.1384 Å (xyz points). All other docking parameters were identical between the two enzymes.

2.7.4. Execution of molecular docking

In this study, AutoDock 1.5.7 was employed to facilitate the docking of *P. thonningii's* compounds to target enzymes, in accordance with a previously documented protocol (Mamoudou, Başaran, et al., 2024; Nganso Ditchou et al., 2024). The ligands and receptors were prepared in PDBQT format, and the grid was configured to permit unrestricted ligand movement. The AutoDock program was executed using the Lamarck Genetic Algorithm (LGA)

as the docking algorithm (Trott & Olson, 2010). A total of 10 poses were generated, and the poses with the optimal energy scores were selected for further analysis.

2.7.5. Output and complexes visualization using PyMOL and Discovery Studio

The output files were saved in the PDBQT format. For the virtual screening studies, we used the crystal structures of porcine pancreatic α-amylase (PDB ID: 4GQR) and yeast α-glucosidase (PDB ID: 2QLY), which are well-established and validated targets for anti-diabetic drug discovery (Aissatou et al., 2025; Hamadou et al., 2025; Mamoudou, Abdoulaye, et al., 2025; Nganso Ditchou et al., 2024). The structures were prepared by removing co-crystallized ligands and water molecules, and adding polar hydrogens and Kollman charges (Trott & Olson, 2010).

The molecular interaction complex was visualized in three-dimensional (3D) and two-dimensional (2D) formats using Discovery Studio 2021 Client software (version 21.1.0.20298).

2.7.6. Dynamics simulation with Desmond

The protein-ligand complexes were subjected to molecular dynamics simulations using Schrödinger's Desmond program. Using the SPC water model, the systems were put inside a 10 Å orthorhombic box that was filled with water. Counter-ions and 0.15 M NaCl were introduced, followed by heating and energy minimization ensure electro-neutrality (Alhagri et al., 2024; Siddiqui et al., 2024). After importing the minimized system into the MD module, the simulation was run for 100 ns under isothermal-isobaric (NPT) conditions, at a temperature of 300 K and a pressure of 1 bar. The Nose-Hoover chain thermostat and the Martyna-Tobias-Klein barostat were used at 100 and 200 ps intervals, respectively, to maintain these parameters (Ipe et al., 2024; Khan et al., 2024; Rathod et al., 2024). Every 100 ps, the simulation was snapped, and the trajectories that resulted were examined.

2.8. Statistical data analysis

All *in vitro* assays, including the antioxidant and anti-diabetic activity measurements, were performed in triplicate (n=3). The data were presented as the mean ± standard deviation (SD). Statistical analyses were conducted using the SPSS 22.0 statistical software and GraphPad Prism 8.0. The data were analyzed using a one-way analysis of variance (ANOVA) to compare differences between groups, followed by Tukey's post-hoc test for multiple comparisons. A p-value of less than 0.05 was considered statistically significant.

3. Results

3.1. NMR identification

Chromatographic fractionation of crude methanolic and ethyl acetate extracts from *P. thonningii* leaves yielded ten known compounds. Structural elucidation was achieved through a combination of spectroscopic analyses (1D-NMR, 2D-NMR, MS, IR) and comparison with literature data.

The isolated compounds (**s**) included 2H-chromen-2-one (Wang et al., 2023), shikimic acid (Bochkov et al., 2012), n-eicosyl trans-ferulate (Chang et al., 2001), epicatechin (Moreira-Araújo et al., 2017), genkwanin (Ijaz et al., 2023), methyl β-D-glucopyranoside (Jeffrey & Takagi, 1977), 3,3',4',5-tetrahydroxystilbene (INAMORI et al., 1984), vitexin (Yutharaksanukul et al., 2024), isorhamnetin 3-O-rutinoside (Boubaker et al., 2011; DOU et al., 2017), and kaempferol 3-O-α-L-rhamnopyranosyl (1-2)-β-D-galactopyranoside (Avanza et al., 2021; DOU et al., 2017; Tsiklauri et al., 2011) (Fig. 3).

3.2. Assessed biological activities: antioxidant and antidiabetic

3.2.1. DPPH antiradical activity

Table 1 illustrates the results of the evaluation of the radical scavenging activity performed on the extracts and its isolated compounds of leaves of *P. thonningii*. The results were expressed as percentage of inhibition. The obtained results experimentally revealed that the inhibition percentage varied significantly from 30.03±0.10% to 71.72±0.62% ($p \leq 0.05$).

The methanolic (MeOH) extract of *P. thonningii* exhibited substantial antioxidant activity, as evidenced by an IC_{50} value of 184.00 µg/mL and 71.72% inhibition. This suggests the presence of compounds with pronounced free radical scavenging capabilities. This activity was comparable to that of the standard antioxidant butylated hydroxytoluene (BHT), which displayed an IC_{50} of 171.81 µg/mL and 74.12% inhibition. In contrast, the ethyl acetate (EtOAc) extract demonstrated a lower antioxidant potency, with an IC_{50} of 281.00 µg/mL and 70.17% inhibition. This suggests that the methanol extraction method captures more potent antioxidant compounds.

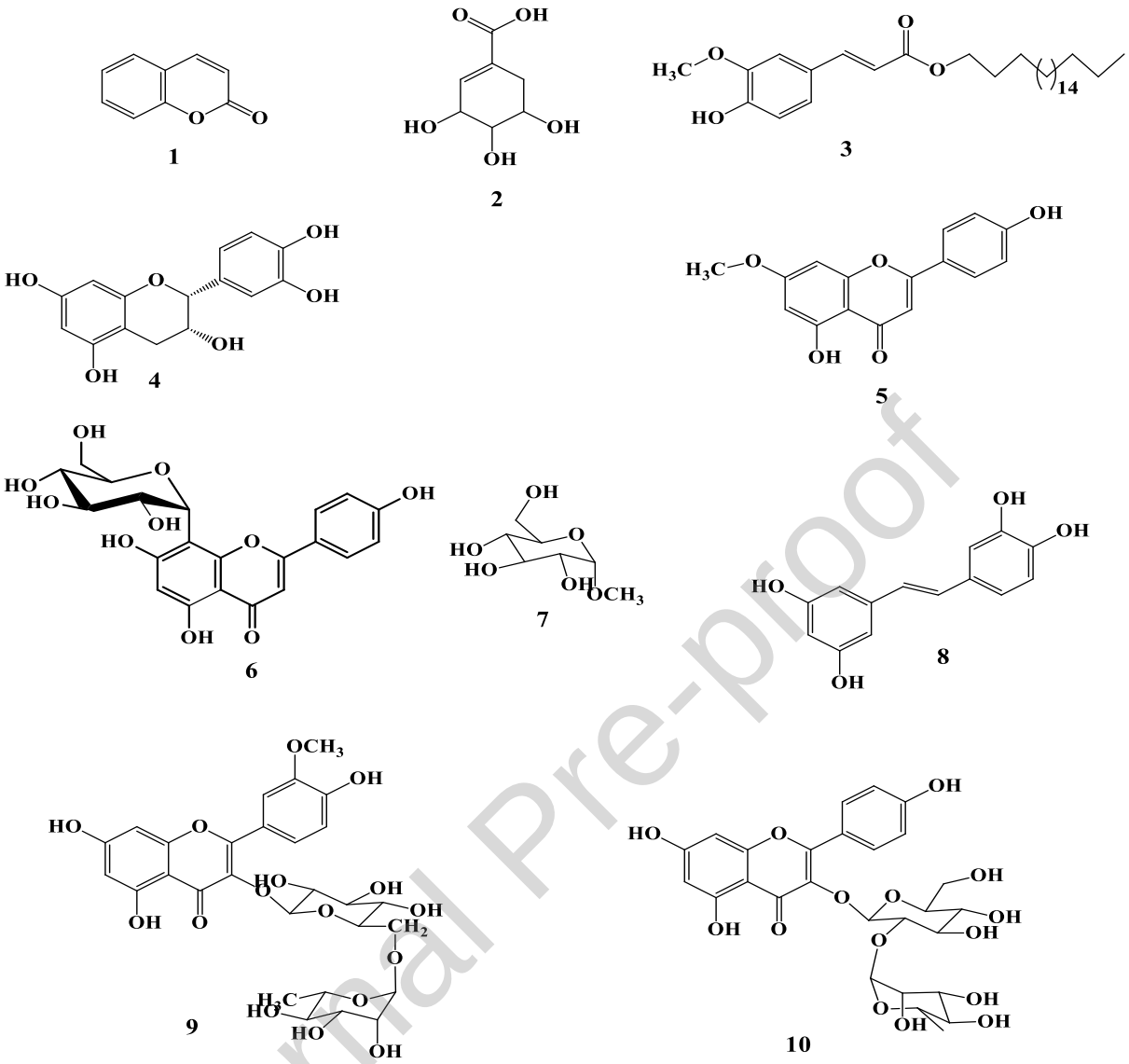

Fig. 3. Structures of compounds isolated from *P. thonningii*

Legend: 1. 2H-chromen-2-one (MW: 146.15 Da). 2. Shikimic acid (MW: 174.15 Da). Moderate α-glucosidase inhibitor. 3. n-eicosyl trans ferrulate (MW: 474.72 Da). 4. Epicatechin (MW: 290.27 Da). Potent α-glucosidase inhibitor. 5. Genkwanin (MW: 284.27 Da). Most potent α-amylase and α-glucosidase inhibitor. 6. Vitexin (MW: 432.38 Da). Strongest binding affinity in molecular docking studies. 7. Methyl β-D-glucopyranoside (MW: 194.19 Da). 8. 3,3',4',5-tetrahydroxystilbene (MW: 244.24 Da). 9. Isorhamnetin 3-O-rutinoside (MW: 624.54 Da). 10. Kaempferol 3-O-α-L-rhamnopyranosyl-(1-2)-β-D-galactopyranoside (MW: 596.52 Da).

Of the isolated compounds, 2H-chromen-2-one (**1**) and shikimic acid (**2**) exhibited moderate antioxidant activity, with IC_{50} values of 208.00 and 297.10 µg/mL, respectively. However, the percentage inhibitions of these compounds (47.52% and 39.83%) were lower in comparison to the methanolic extract. Epicatechin (**4**) exhibited relatively strong antioxidant properties (IC_{50}: 300.35 µg/mL), however, its inhibition percentage (30.40%) was significantly lower ($p \leq 0.05$).

Derivatives of kaempferol, in particular kaempferol 3-O-α-L-rhamnopyranosyl-(1-2)-β-D-galactopyranoside (**10**), exhibited notable antioxidant potential, with an IC_{50} of 172.45 µg/mL and 69.48% inhibition, indicative of robust free radical scavenging properties. Methyl β-D-glucopyranoside (**7**) and 3,3',4′,5-tetrahydroxystilbene (**8**) demonstrated moderate antioxidant activity, with IC_{50} values of 184.85 and 177.41 µg/mL, respectively.

The findings indicate that the methanol extract of *P. thonningii* exhibits promising antioxidant potential, comparable to that of the synthetic antioxidant BHT. The observed variability in antioxidant activity among the isolated compounds underscores the significance of solvent selection in extracting bioactive compounds. Notably, kaempferol derivatives emerge as potent natural antioxidants, a finding that aligns with previous research (Avanza et al., 2021; Kabré et al., 2023; Mamoudou & Mune, 2025; Tsiklauri et al., 2011).

3.2.2. ABTS free radical scavenging activity

The ability of extracts and isolated compounds from the leaves of the species *P. thonningii* to trap free radicals was recorded in the table below (Table 1) and expressed as percentage of trapping. In general, the $ABTS^{+}$ antiradical activity of the tested samples was also important with trapping percentages ranging from 36.14±0.12% to 69.26±0.29% ($p \leq 0.05$). The methanol (MeOH) extract of *P. thonningii* demonstrated exceptional antioxidant activity, with an IC_{50} value of 181.05 ± 1.91 µg/mL and 69.26 ± 0.29% inhibition, closely rivalling the standard antioxidant butylated hydroxytoluene (BHT; IC_{50} = 173.75 ± 2.19 µg/mL, 72.02 ± 1.11%). This potent activity suggests the presence of highly effective antioxidant constituents capable of scavenging 2,2'-azino-bis (3-ethylbenzothiazoline-6-sulphonic acid) (ABTS) radicals. In contrast, the ethyl acetate (EtOAc) extract exhibited moderate antioxidant activity (IC_{50} = 197.11 ± 1.27 µg/mL, 62.94 ± 0.51% inhibition), implying differences in antioxidant composition, potentially lower levels of phenolic compounds or flavonoids.

Among the isolated compounds, kaempferol 3-O-α-L-rhamnopyranoside (**10**) displayed the highest antioxidant activity (IC_{50} = 175.61 ± 1.41 µg/mL, 57.92 ± 0.45% inhibition), consistent with kaempferol's established radical-scavenging properties. Isorhamnetin 3-O-rutinoside (**9**) also demonstrated notable antioxidant activity (IC_{50} = 184.85 ± 0.92 µg/mL, 55.19 ± 0.63% inhibition), highlighting its therapeutic potential in mitigating oxidative stress. Methyl β-D-glucopyranoside (**7**) exhibited moderate antioxidant activity (IC_{50} = 174.55 ± 2.75 µg/mL, 51.71 ± 0.84% inhibition), while shikimic acid (**2**) and epicatechin (**4**) displayed relatively lower

activities (IC_{50} values of 176.51 ± 2.12 µg/mL and 188.45 ± 1.34 µg/mL, respectively). The weakest activity was observed for 3,3',4',5-tetrahydroxystilbene (**8**; IC_{50} = 202.61 ± 1.98 µg/mL, 38.41 ± 0.91% inhibition).

The results of the ABTS assay underscore the substantial antioxidant potential of *P. thonningii* extracts and isolated compounds, particularly the methanol extract and kaempferol 3-O-α-L-rhamnopyranoside (**10**). These findings suggest the presence of bioactive compounds capable of neutralizing free radicals, warranting further investigation into their mechanisms and potential synergistic effects for the development of therapeutic agents against oxidative stress-related diseases.

3.2.3. Ferric-Reducing Antioxidant Power (FRAP)

The reducing power of the crude extracts and isolated compounds is presented in the table (Table 1) and expressed as reducing percentage. According to this table, it appears that the ability of the samples (extracts and compounds) to facilitate the ability of a compound to reduce ferric ions (Fe^{3+}) to ferrous ions (Fe^{2+}) (Benzie & Strain, 1996) varied from 35.23±0.98% to 72.72±0.37%. The higher the FRAP value, the greater the antioxidant activity.

The results show that the MeOH extract and EtOAc extract of *P. thonningii* had the highest FRAP values, with 72.72±0.37% and 70.12±0.745%, respectively. These values are significantly higher than the standard antioxidant BHT, indicating that the crude extracts of *P. thonningii* possess strong antioxidant activity.

Among the individual compounds, the compound 3,3',4',5-tetrahydroxystilbene (**8**) exhibited the highest FRAP value (61.08±0.49%), followed by methyl β-D-glucopyranoside (**7**) (65.97±0.74%), and genkwanin (**5**) (63.55±0.12%). These compounds also showed significant antioxidant activity compared to the standard BHT.

The FRAP values of the other compounds, such as shikimic acid (**2**), n-eicosyl trans ferrulate (**3**), epicatechin (**4**), vitexin (**6**), isorhamnetin 3-O-rutinoside (**9**), and kaempferol 3-O-α-L-Rhamnopyranosyl (1-2)-β-D-galactopyranoside (**10**) were also notable, indicating that these compounds also possess antioxidant activity.

The results of this study suggest that *P. thonningii* is a rich source of antioxidants, particularly its crude extracts and compounds such as 3,3',4',5-tetrahydroxystilbene (**8**), methyl β-D-glucopyranoside (**7**), and genkwanin (**5**). These findings support the potential of *P. thonningii*

as a natural source of antioxidants with potential applications in various fields, including food, medicine, and cosmetics (Adewole et al., 2024; Huang et al., 2005; Mamoudou, Obadias, et al., 2024; Mamoudou & Mune Mune, 2024; Raimi et al., 2024).

3.2.4. Hydroxyl Radical Scavenging Activity (HRSA)

Table 1 illustrates the antioxidant activity of *P. thonningii* crude extracts and compounds, as determined through the HRSA (Hydroxyl Radical Scavenging Activity) assay. The results are expressed as IC_{50} values (µg/mL) and percentage inhibition. The IC_{50} value represents the concentration of the sample required to inhibit 50% of the free radical activity. Thus, the higher the percentage inhibition, the stronger the antioxidant activity. The scavenging activity of extracts and compounds exhibited a significant increase between 39.55 ± 0.43% and 74.73 ± 0.63%.

The methanol extract of *P. thonningii* exhibited superior antioxidant activity, with an IC_{50} value of 183.51 ± 2.12 µg/mL and a percentage inhibition of 74.73 ± 0.63%, comparable to the standard antioxidant butylated hydroxytoluene (BHT; 174.50 ± 3.54 µg/mL, 75.05 ± 1.67% inhibition). This potent antioxidant capacity suggests a significant ability to neutralize free radicals. The ethyl acetate (EtOAc) extract also demonstrated notable antioxidant activity (IC_{50}: 210.31 ± 3.25 µg/mL, 72.99 ± 0.61% inhibition), indicating the presence of highly active antioxidant compounds in the plant's polar fractions.

Table 1 Antioxidant activities (DPPH, ABTS, HRSA, and FRAP) of *P. thonningii's* crude extracts (MeOH and EtOAc) and isolated compounds

Samples	DPPH		ABTS		HRSA		FRAP
	IC_{50} (µg/mL) [95% CI]	% inhibition	IC_{50} (µg/mL) [95% CI]	% inhibition	IC_{50} (µg/mL) [95% CI]	% inhibition	% inhibition
Extracts							
MeOH	184.00 ± 2.54 [177.69–190.31]^{g}	71.72±0.62^{bc}	181.05 ± 1.91 [176.30–185.80]^{e}	69.26±0.29^{b}	183.51 ± 2.12 [178.24–188.78]^{f}	74.73±0.63^{a}	72.72±0.37^{a}
EtOAc	281.00 ± 2.83 [273.97–288.03]^{h}	70.17±0.88^{c}	197.11 ± 1.27 [193.95–200.27]^{b}	62.94±0.51^{c}	210.31 ± 3.25 [202.24–218.38]^{b}	72.99±0.61^{b}	70.12±0.74^{b}
Compounds							
1	208.00 ± 2.83 [200.97–215.03]^{e}	47.52±0.37^{f}	197.85 ± 1.63 [193.80–201.90]^{b}	47.11±0.63^{h}	195.25 ± 1.34 [191.92–198.58]^{d}	48.31±0.85^{g}	50.49±0.36^{h}
2	297.10 ± 3.54 [288.31–305.89]^{a}	39.83±0.81^{i}	176.51 ± 2.12 [171.24–181.78]^{fg}	38.24±0.26^{j}	194.00 ± 2.83 [186.97–201.03]^{d}	43.61±0.90^{i}	47.13±0.25^{i}

3	203.51 ± 2.12 [198.24–208.78]^{dc}	40.67±0.24^{i}	175.05 ± 1.34 [171.72–178.38]^{fg}	45.54±0.33^{i}	198.35 ± 2.62 [191.84–204.86]^{c}	41.90±1.54^{jh}	58.01±0.50^{g}
4	300.35 ± 2.33 [295.46–305.24]^{a}	30.03±0.10^{k}	188.45 ± 1.34 [185.12–191.78]^{c}	36.14±0.12^{k}	240.41 ± 2.97 [233.80–247.02]^{a}	39.55±0.43^{h}	44.43±0.25^{j}
5	200.00 ± 1.41 [196.50–203.50]^{e}	43.34±0.45^{h}	177.25 ± 1.77 [174.07–180.43]^{f}	48.85±0.36^{g}	175.51 ± 2.12 [170.24–180.78]^{g}	52.07±0.38^{f}	63.55±0.12^{e}
6	196.51 ± 2.12 [191.24–201.78]^{f}	33.28±0.15^{j}	175.21 ± 3.11 [169.52–180.90]^{fg}	45.41±0.36^{i}	192.75 ± 3.61 [184.82–200.68]^{d}	43.53±0.90^{i}	35.23±0.98^{k}
7	184.85 ± 1.63 [181.79–187.91]^{g}	45.27±0.79^{g}	174.55 ± 2.75 [169.57–179.53]^{fg}	51.71±0.38^{f}	194.81 ± 3.39 [187.06–202.56]^{d}	58.14±1.32^{e}	65.97±0.74^{d}
8	177.41 ± 2.26 [172.92–181.90]^{h}	47.49±0.26^{f}	202.61 ± 1.98 [198.16–207.06]^{a}	38.41±0.91^{j}	210.35 ± 2.47 [205.48–215.22]^{b}	45.81±0.96^{h}	61.08±0.49^{f}
9	175.25 ± 1.77 [172.07–178.43]^{h}	58.55±1.59^{e}	184.85 ± 0.92 [182.57–187.13]^{d}	55.19±0.63^{e}	186.45 ± 2.19 [181.30–191.60]^{ef}	65.13±0.78^{d}	69.37±0.50^{c}
10	172.45 ± 0.078 [172.33–172.57]^{i}	69.48±0.58^{d}	175.61 ± 1.41 [172.11–179.11]^{fg}	57.92±0.45^{d}	176.05 ± 3.61 [168.12–183.98]^{g}	67.97±0.83^{c}	68.97±0.85^{c}
Standard							
BHT	171.81 ± 2.54 [165.50–178.12]^{i}	74.12±0.92^{a}	173.75 ± 2.19 [168.60–178.90]^{g}	72.02±1.11^{a}	174.50 ± 3.54 [166.69–182.31]^{g}	75.05±1.67^{a}	-

Values with the same letter are not significantly different at p>0.05.
Legend: *2H-chromen-2-one (**1**), Shikimic acid (**2**), n-eicosyl trans ferrulate (**3**), Epicatechin (**4**), Genkwanin (**5**), Vitexin (**6**), Methyl β-D-glucopyranoside (7), 3,3',4',5-tetrahydroxystilbene (**8**), Isorhamnetin 3-O-rutinoside (**9**), Kaempferol 3-O-α-L-Rhamnopyranosyl (1-2)-β-D-galactopyranoside (**10**); DPPH: 2,2- diphenyl-1-picrylhydrazyl; ATBS: 2,2-azino-bis (3-ethylbenzylthiozoline-6-sulphonic acid); HRSA: Hydroxyl Radical Scavenging Activity; FRAP: Ferric-reducing antioxidant power*

Notably, individual compounds exhibited substantial antioxidant activities. Kaempferol 3-O-α-L-Rhamnopyranoside (**10**) displayed the highest radical scavenging activity (IC_{50}: 176.05 ± 3.61 µg/mL, 67.97 ± 0.83% inhibition), rivaling BHT, consistent with the established strong antioxidant properties of flavonoids. Methyl β-D-glucopyranoside (**7**) also showed significant antioxidant potential (IC_{50}: 194.81 ± 3.39 µg/mL, 58.14 ± 1.32% inhibition), likely attributed to its structural capacity for free radical scavenging. Other compounds, including isorhamnetin 3-O-rutinoside (**9**) and genkwanin (**5**), demonstrated moderate antioxidant activities (IC_{50} values: 186.45 ± 2.19 µg/mL and 175.51 ± 2.12 µg/mL, respectively).

In contrast, shikimic acid (**2**) and epicatechin (**4**) exhibited relatively lower antioxidant activities (IC_{50} values: 194.00 ± 2.83 µg/mL and 240.41 ± 2.97 µg/mL, % inhibition: 43.61 ± 0.90% and 39.55 ± 0.43%, respectively), suggesting they may not primarily contribute to the crude extracts' antioxidant properties.

The observed antioxidant capacities of *P. thonningii* extracts and isolated compounds, particularly kaempferol 3-O-α-L-rhamnopyranoside, underscore their potential health benefits and therapeutic applications. These findings emphasize the importance of exploring plant extracts and isolated compounds for their radical scavenging abilities, which could provide valuable strategies for combating oxidative stress-related diseases.

3.2.5. *P. thonningii's* compounds as α-amylase inhibitors

Fig. 4 presents data illustrating the inhibitory effects of various extracts and compounds on α-amylase activity, a crucial enzyme in carbohydrate digestion. The IC_{50} values and corresponding percentage inhibitions serve as vital indicators of the therapeutic potential of these substances in the management of postprandial hyperglycemia, particularly in the context of diabetes.

It is noteworthy that the methanol (MeOH) extract exhibited the lowest IC_{50} value (184.45 ± 1.21 µg/mL), accompanied by a significant inhibition percentage (74.09 ± 0.36%). This indicates that the methanol (MeOH) extract is an effective α-amylase inhibitor, which is likely due to its high concentration of phytochemicals. The ethyl acetate (EtOAc) extract exhibited notable activity, with an IC_{50} of 194.05 ± 1.77 µg/mL and a percentage inhibition of 69.92 ± 0.24%.

Among the tested compounds, genkwanin displayed promising inhibitory activity, with an IC_{50} value of 180.95 ± 2.19 µg/mL and an inhibition percentage of 64.52 ± 0.25%. In contrast, shikimic acid and n-eicosyl trans ferrulate demonstrated higher IC_{50} values (307.91 ± 3.54 µg/mL and 202.91 ± 3.39 µg/mL, respectively) and lower inhibition percentages (45.52 ± 0.37% and 49.04 ± 0.37%). These results highlight the significant variability in compound efficacy.

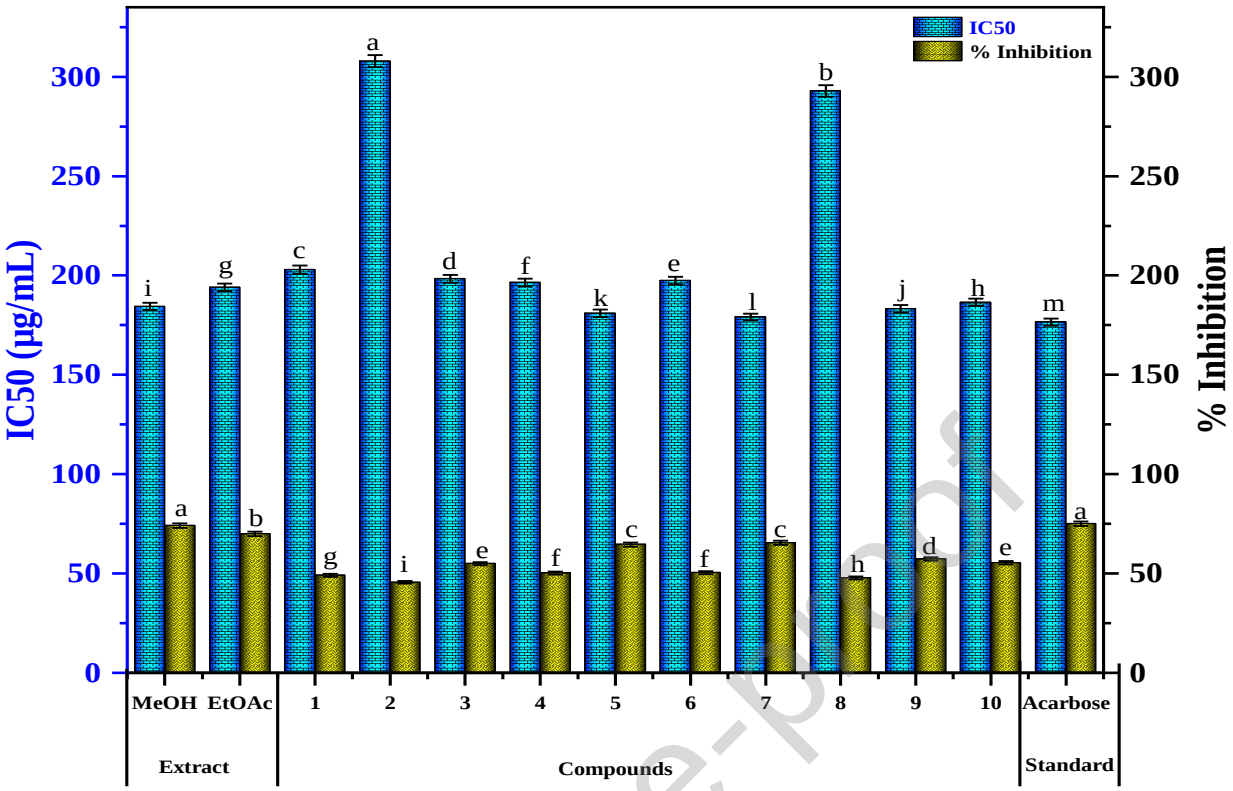

Fig. 4. Antidiabetic activity of *P. thonnigii's* crude extract and isolated compounds against α-amylase

Legend: *2H-chromen-2-one (**1**), Shikimic acid (**2**), n-eicosyl trans ferrulate (**3**), Epicatechin (**4**), Genkwanin (**5**), Vitexin (**6**), Methyl β-D-glucopyranoside (**7**), 3,3',4',5-tetrahydroxystilbene (**8**), Isorhamnetin 3-O-rutinoside (**9**), Kaempferol 3-O-α-L-Rhamnopyranosyl (1-2)-β-D-galactopyranoside (**10**)*

Results with the same letter are not significantly different at p>0.05.

The standard α-amylase inhibitor, acarbose, displayed an IC_{50} of 176.51 ± 2.12 µg/mL. This value serves as a benchmark for comparison. Notably, the methanolic (MeOH) extract (IC_{50} = 184.45 µg/mL) and the isolated compound genkwanin (IC_{50} = 180.95 µg/mL) exhibited IC_{50} values that are highly comparable to that of acarbose. To provide a clearer context, genkwanin demonstrated a relative potency of 97.5% compared to acarbose (calculated as IC_{50} of acarbose / IC_{50} of genkwanin), indicating a very similar level of inhibitory activity. These findings indicate that the MeOH extract and specific compounds, such as genkwanin, have the potential to serve as potent α-amylase inhibitors for the management of blood glucose levels.

3.2.5. *P. thonningii's* compounds as α-glucosidase inhibitors

The inhibitory effects of various extracts and compounds on α-glucosidase activity, a crucial enzyme in carbohydrate metabolism, is shown in Fig. 5. The IC_{50} values and percentage inhibition provide essential metrics for evaluating the potential of these substances as α-

glucosidase inhibitors, particularly in the context of postprandial hyperglycemia management in diabetes.

The methanolic (MeOH) extract exhibited the lowest IC_{50} value (175.61 ± 0.85 μg/mL), corresponding to a 73.01 ± 0.38% inhibition rate. This indicates that the bioactive compounds in the extract are capable of interacting effectively with the enzyme, which may be responsible for the significant inhibitory activity observed. In contrast, the ethyl acetate (EtOAc) extract exhibited a slightly higher IC50 value (186.31 ± 2.41 μg/mL) and 67.23 ± 0.37% inhibition.

Among the individual compounds, shikimic acid demonstrated moderate activity, with an IC_{50} value of 196.25 ± 2.47 μg/mL and an inhibition rate of 47.77 ± 0.38%. Notable inhibitory effects were observed for epicatechin and genkwanin, with IC_{50} values of 201.51 ± 2.12 μg/mL and 174.95 ± 2.05 μg/mL, respectively. The higher inhibition percentage exhibited by genkwanin (63.55 ± 0.26%) indicates the potential for it to function as a more effective inhibitor.

Acarbose, a conventional α-glucosidase inhibitor, exhibited an IC_{50} of 171.15 ± 1.63 μg/mL. This benchmark underscores the potential of the evaluated extracts and compounds as alternative or complementary agents. Genkwanin exhibited an IC_{50} of 174.95 ± 2.05 μg/mL, indicating an inhibitory potency comparable to that of acarbose. Genkwanin demonstrated a relative potency of 97.8% in comparison to acarbose, as determined by the ratio of the IC_{50} values (IC_{50} of acarbose / IC_{50} of genkwanin), indicating its effectiveness is comparable to the clinical standard on a mass basis. The results suggest that the MeOH extract and genkwanin are viable candidates for further exploration in the development of α-glucosidase inhibitors.

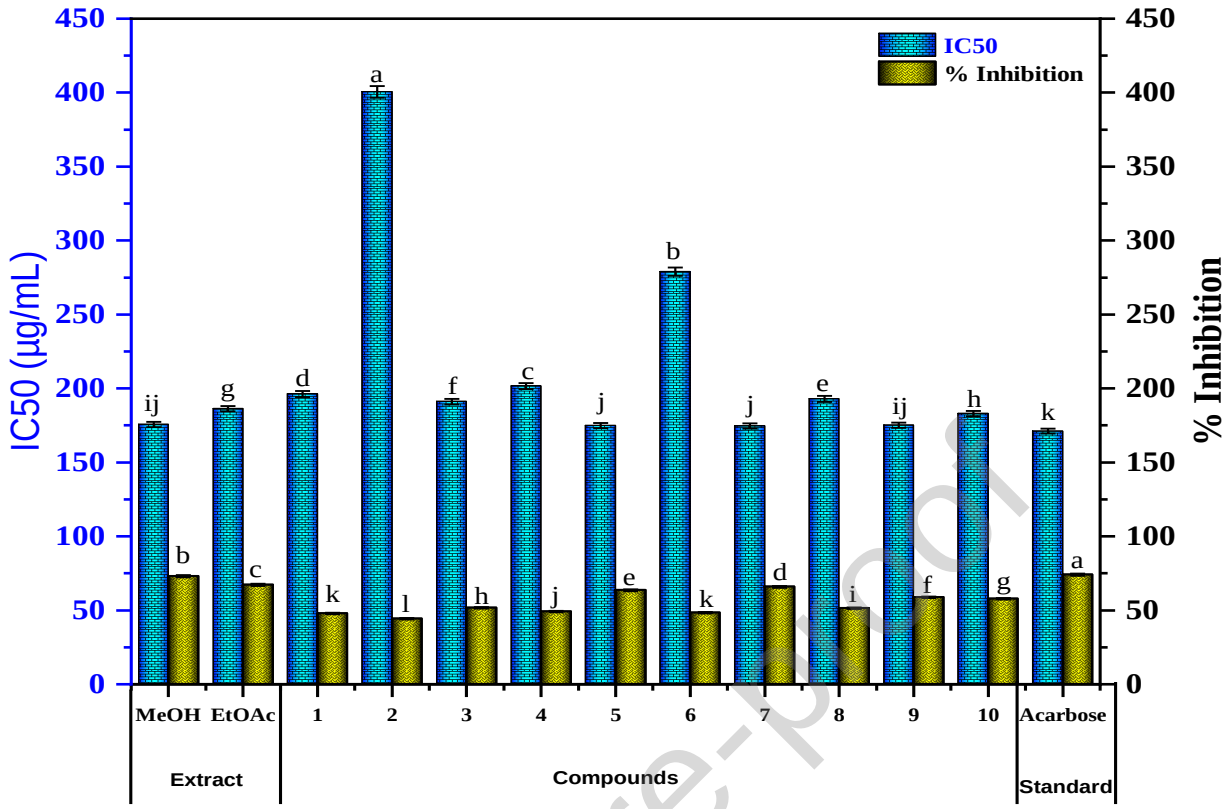

Fig. 5. Antidiabetic activity of *P. thonnigii's* crude extract and isolated compounds against α-glucosidase

Legend: *2H-chromen-2-one (**1**), Shikimic acid (**2**), n-eicosyl trans ferrulate (**3**), Epicatechin (**4**), Genkwanin (**5**), Vitexin (**6**), Methyl β-D-glucopyranoside (**7**), 3,3',4',5-tetrahydroxystilbene (**8**), Isorhamnetin 3-O-rutinoside (**9**), Kaempferol 3-O-α-L-Rhamnopyranosyl (1-2)-β-D-galactopyranoside (**10**)*

Results with the same letter are not significantly different at p>0.05.

3.3. Binding affinity and molecular docking interactions

3.3.1. Protein-ligand binding affinity prediction

The analysis of binding energies for the ten compounds isolated from *Piliostigma thonningii* in relation to the enzyme's α-amylase and α -glucosidase (Table 2) provides significant insights into their potential antidiabetic properties. Binding affinity, measured in kilocalories per mole (kcal/mol), serves as a critical indicator of the strength of interaction between these compounds and the target enzymes, which play pivotal roles in carbohydrate metabolism and glucose regulation.

Table 2 Binding affinity between *P. thonningii's* compounds and antidiabetic enzyme targets

Ligand	**Binding Affinity (kcal/mol)**

	α-amylase	**α-glucosidase**
2H-chromen-2-one (**1**)	-5.8	-6.6
shikimic acid (**2**)	-5.5	-6.5
n-eicosyl trans ferrulate (**3**)	-6.2	-7.3
Epicatechin (**4**)	-8.3	-8.2
Genkwanin (**5**)	-8.5	-8.1
Vitexin (**6**)	-8.6	-8.5
methyl β-D-glucopyranoside (**7**)	-5.2	-5.4
3,3',4',5-tetrahydroxystilbene (**8**)	-7.5	-7.4
isorhamnetin 3-O-rutinoside (**9**)	-6.1	-9.1
kaempferol 3-O-α-L-rhamnopyranosyl (1-2)-β-D-galactopyranoside (**10**)	-7.7	-8.1
Acarbose (reference drug)	-7.0	-7.0

Among the compounds studied, vitexin (**6**) exhibited the highest binding affinity for both α-amylase (-8.6 kcal/mol) and α-glucosidase (-8.5 kcal/mol). This suggests that Vitexin may effectively inhibit these enzymes, thereby reducing the breakdown of carbohydrates into glucose and potentially lowering postprandial blood glucose levels. Epicatechin (**4**) also demonstrated strong binding affinities (-8.3 kcal/mol for α-amylase and -8.2 kcal/mol for α-glucosidase), indicating its potential as a therapeutic agent in managing diabetes through similar mechanisms.

In contrast, methyl β-D-glucopyranoside (**7**) and shikimic acid (**2**) showed lower binding affinities (-5.2 and -5.5 kcal/mol for α-amylase, respectively), suggesting a weaker interaction with the enzymes. This may limit their effectiveness as antidiabetic agents compared to the more potent compounds. The compound 2H-chromen-2-one (**1**) and 3,3',4',5-tetrahydroxystilbene (**8**) also displayed moderate binding affinities (-5.8 and -7.5 kcal/mol for α-amylase, respectively), indicating potential but less pronounced inhibitory effects.

Genkwanin (**5**) and n-eicosyl trans ferulate (**3**) had binding affinities of -8.5 and -6.1 kcal/mol for α-amylase, respectively, with Genkwanin also showing a notable affinity for α-glucosidase (-8.1 kcal/mol). These results suggest that both compounds may contribute to antidiabetic effects, although further investigation is warranted to elucidate their mechanisms of action.

The compound kaempferol 3-O-α-L-rhamnopyranosyl (1-2)-β-D-galactopyranoside (**10**) exhibited a binding affinity of -7.7 kcal/mol for α-amylase and -8.1 kcal/mol for α-glucosidase, indicating a promising potential for glucose regulation. Conversely, Acarbose, a well-known reference drug, demonstrated a binding affinity of -7.0 kcal/mol for both enzymes, which, while effective, is lower than that of several compounds isolated from *Piliostigma thonningii*.

Overall, the binding affinity data suggest that compounds such as vitexin (**6**) and epicatechin (**4**) may serve as effective inhibitors of α-amylase and α-glucosidase, thereby offering potential therapeutic benefits in the management of diabetes. The varying affinities highlight the importance of structural characteristics in determining enzyme interactions, warranting further exploration of these compounds' mechanisms and their efficacy in clinical situations.

3.3.2. Molecular level interactions a-amylase-ligand

Molecular docking studies provide valuable insights into the interactions between small molecules and target enzymes, which is crucial for understanding their potential therapeutic applications. In the case of genkwanin (**5**) (Fig. 6A), a flavonoid compound, its docking with the α-amylase enzyme reveals significant binding interactions that may elucidate its role in antidiabetic activity. The docking analysis highlights key interactions, including van der Waals, particularly with residues such as His101, Glu233, and Arg195. These interactions are essential for the inhibition of α-amylase, as they can disrupt the enzyme's catalytic function, thereby reducing the breakdown of carbohydrates into glucose and contributing to lower blood sugar levels (Brayer et al., 1995; Ibrahim et al., 2018; Mudgil et al., 2024; Nganso Ditchou et al., 2024; Núñez et al., 2023; Tiwari et al., 2023; Wongsa et al., 2023) Furthermore, the presence of specific functional groups in these compounds likely contributes to their binding efficacy, as they can engage in various interactions, including van der Waals forces and pi-stacking interactions. For instance, compounds that form stable interactions with key residues such as Asp300 and Tyr62 in α-amylase may exhibit enhanced inhibitory effects. The implications of these findings are profound, as they not only support the traditional use of *Piliostigma thonningii* in diabetes management but also pave the way for the development of novel antidiabetic agents based on these natural compounds.

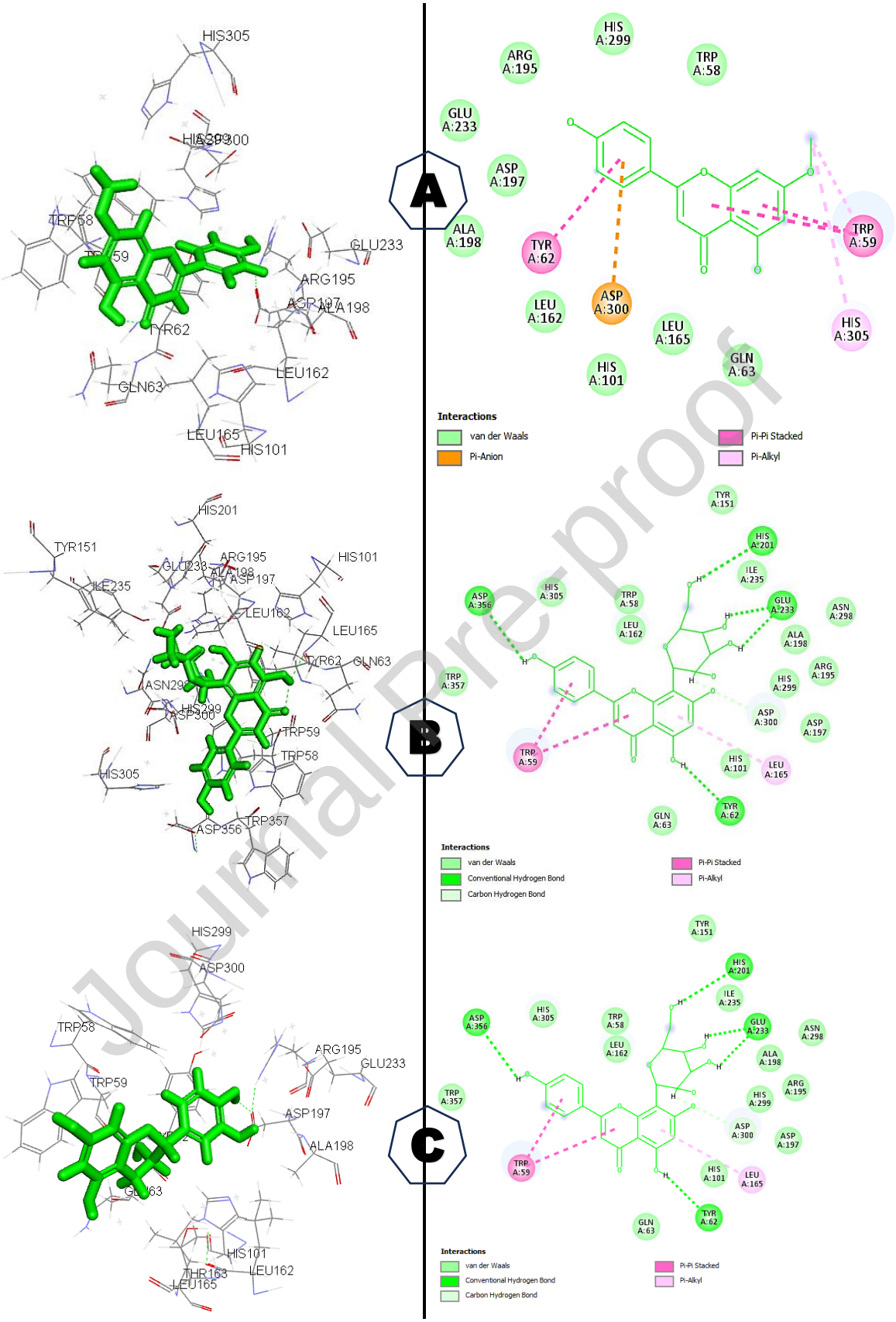

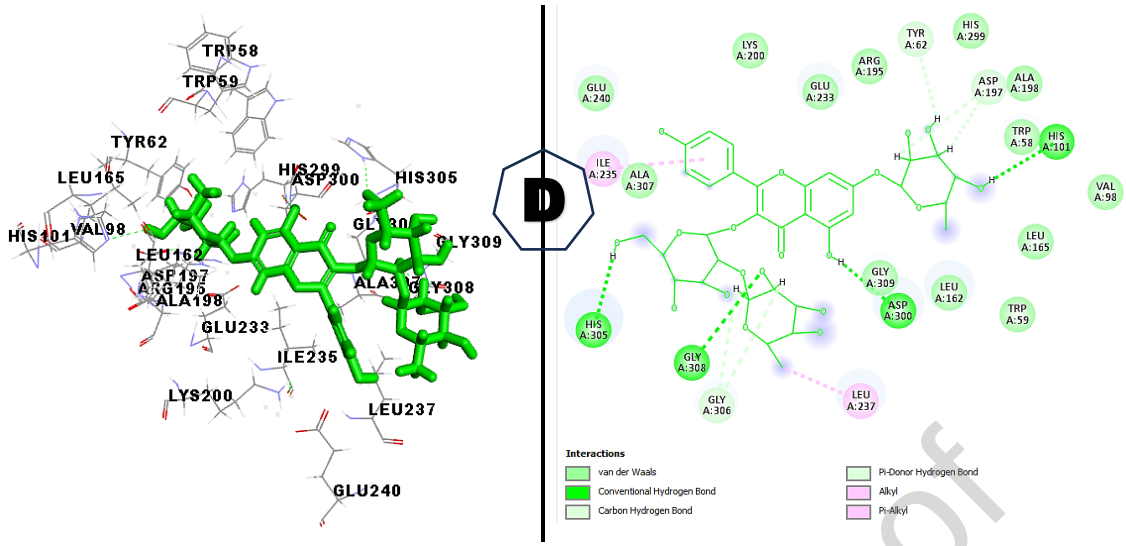

Fig. 6. Visualization of molecular interactions between Genkwanin (A), Vitexin (B), Epicatechin (C), kaempferol 3-O-α-L-Rhamnopyranosyl (1-2)-β-D-galactopyranoside (D) and a-amylase

The molecular docking results between vitexin (**6**) and the α-amylase enzyme, as depicted in Fig. 6B, suggest several significant interactions between the ligand (vitexin) and key residues in the active site of the enzyme. Key hydrogen bond interactions include those between vitexin (**6**) and residues like HIS A:299, ASP A:300, and LEU A:241. These hydrogen bonds are crucial as they enhance the binding affinity of vitexin by stabilizing its position and potentially blocking the substrate from accessing the catalytic site. Additionally, the interaction with LEU A:241 might be involved in hydrophobic stabilization, further anchoring the compound. In addition, the van der Waals interactions, such as those with TRP A:59 and HIS A:201, contribute to the overall binding stability but are weaker compared to hydrogen bonds. Notably, the presence of pi-stacking (with TRP A:59) and pi-alkyl interactions indicates that vitexin interacts with aromatic residues, which can play a role in binding by stabilizing the planar structure of vitexin against the side chains of these residues. From the docking diagram, vitexin (**6**) engages in multiple types of interactions with the amino acid residues of α-amylase, including conventional hydrogen bonds, carbon-hydrogen bonds, van der Waals forces, and pi-related interactions (such as pi-stacked and pi-alkyl). The majority of these interactions appear to stabilize the ligand within the enzyme's active site, which likely influences the enzyme's catalytic activity.

The docking results between epicatechin (**4**) and the α-amylase enzyme (Fig. 6C) illustrate a range of interactions that suggest epicatechin's potential inhibitory effect on the enzyme. Conventional hydrogen bonds are observed with residues ASP A:197 and GLN A:63, which are critical for maintaining the orientation of epicatechin within the active site. Additionally, pi-pi

stacking interactions with residues TRP A:58 and TYR A:62 further stabilize epicatechin (**4**) by exploiting the aromatic nature of these residues, which likely enhances the affinity of the compound for α-amylase. Epicatechin (**4**) appears to interact favorably with key residues in the α-amylase active site, particularly through hydrogen bonds and pi-pi stacking.

The molecular interaction analysis kaempferol 3-O-α-L-rhamnopyranosyl (1-2)-β-D-galactopyranoside (**10**) and α-amylase (Fig. 6D) reveals several interactions that contribute to its binding affinity and potential inhibitory effects on α-amylase. The docking results indicate that the compound forms multiple hydrogen bonds and van der Waals interactions with key amino acid residues in the active site of α-amylase. Notably, residues such as His305, Asp300, and Gly308 are involved in conventional hydrogen bonding, which stabilizes the ligand-enzyme complex. The presence of these interactions suggests that kaempferol 3-O-α-L-rhamnopyranosyl (1-2)-β-D-galactopyranoside (**10**) may effectively inhibit α-amylase activity by blocking the substrate binding site, thereby reducing the enzyme's ability to hydrolyze starch into glucose. Additionally, the analysis highlights the role of hydrophobic interactions, particularly with residues like Leu162 and Val98, which further enhance the binding stability of the ligand. The combination of these interactions indicates a strong affinity of the compound for the enzyme, suggesting its potential as a natural inhibitor of α-amylase.

The molecular docking elucidates the mechanism of action of these compounds and supports their potential therapeutic applications in managing conditions related to carbohydrate metabolism, such as diabetes.

3.3.3. Molecular level interactions a-glucosidase-ligand

Molecular docking simulations between kaempferol 3-O-α-L-rhamnopyranosyl (1-2)-β-D-galactopyranoside (**10**) and α-glucosidase enzyme (Fig. 7A) revealed intricate binding interactions, shedding light on the compound's potential inhibitory effects. The docking results exhibited a complex interplay of hydrogen bonds, van der Waals forces, and unfavorable interactions, collectively influencing ligand binding affinity and specificity. Notably, hydrogen bonding between kaempferol's hydroxyl groups and key amino acid residues, such as ARG (A: 730) and GLU (A: 661), indicated strong affinity and optimal ligand positioning within the active site. Conventional hydrogen bonds reinforced these favorable interactions, essential for effective enzyme inhibition. Conversely, unfavorable interactions involving GLU (A: 767) and ARG (A: 643) may compromise optimal binding, suggesting targeted ligand modifications to

enhance binding efficiency. Van der Waals interactions provided additional stabilization, contributing to the overall binding energy.

This docking study demonstrates that kaempferol 3-O-α-L-rhamnopyranosyl (1-2)-β-D-galactopyranoside (**10**) exhibits a promising binding profile with α-glucosidase, characterized by a balance of favorable and unfavorable interactions. These findings underscore the compound's potential as an α-glucosidase inhibitor and highlight the need for further structural optimization to augment its therapeutic efficacy.

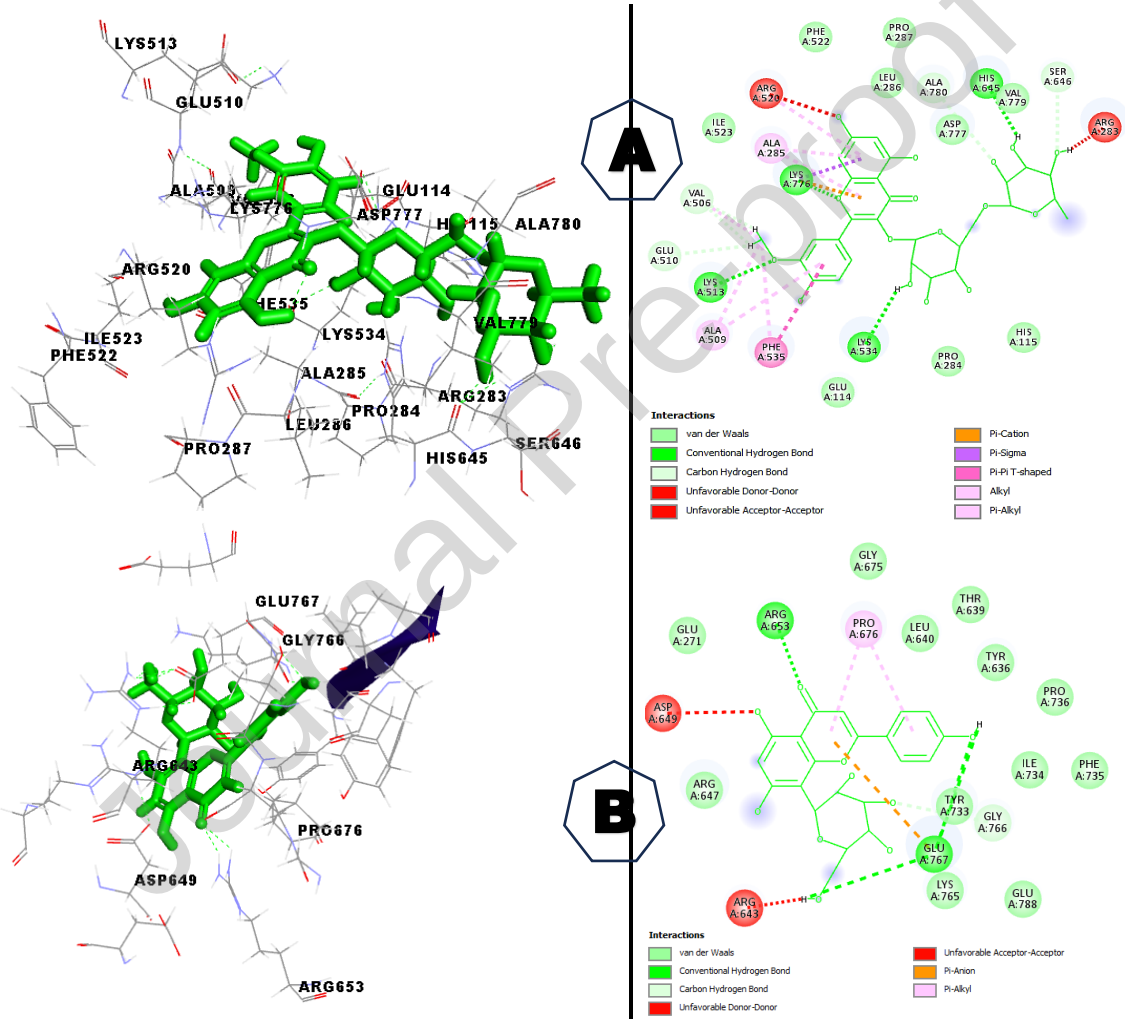

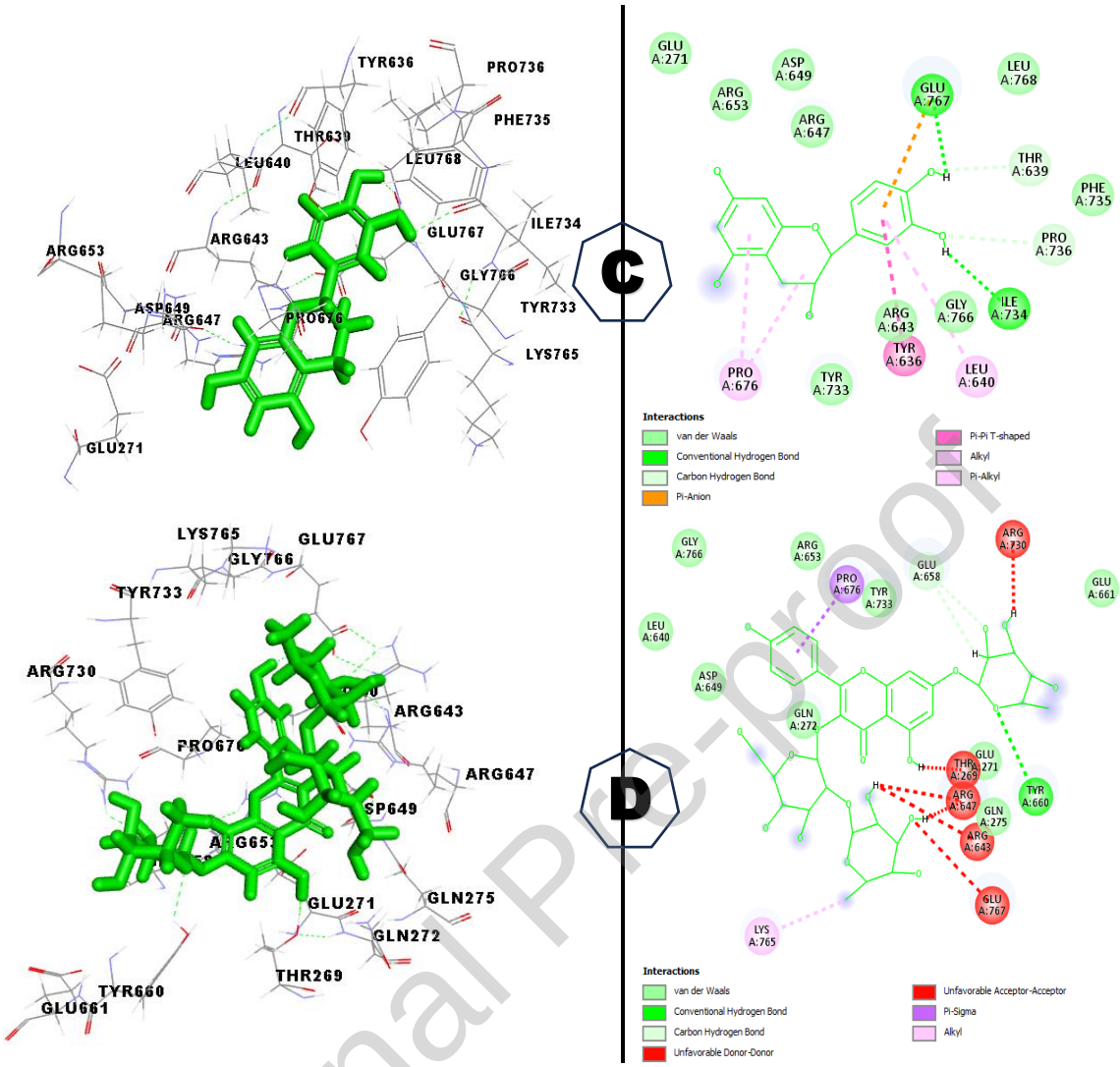

Fig. 7. Visualization of molecular interactions between kaempferol 3-O-α-L-rhamnopyranosyl (1-2)-β-D-galactopyranoside (A), Vitexin (B), Epicatechin (C), isorhamnetin 3-O-rutinoside (D) and a-glucosidase

The Fig. 7B depicts a molecular docking analysis of vitexin (**6**) and α-glucosidase. The results suggest that vitexin (**6**) binds to the enzyme through a network of interactions, including van der Waals forces, conventional hydrogen bonds, and pi-alkyl interactions. Notably, vitexin (**6**) engages with several amino acid residues within the active site, including Arg 643, Glu 271, Arg 653, Pro 676, Glu 767, Tyr 733, and Lys 765. Arg 643 participates in an unfavorable donor-donor interaction, while Glu 271 and Arg 653 form conventional hydrogen bonds with vitexin. Pro 676 and Glu 767 engage in Pi-Alkyl and Pi-Anion interactions, respectively. Additionally, Tyr 733 interacts through van der Waals forces, and Lys 765 contributes another conventional hydrogen bond. These interactions collectively suggest that vitexin binds to the active site of α-glucosidase, potentially acting as a competitive inhibitor. This binding mode could hinder the enzyme's catalytic activity by blocking the substrate from accessing the active site. This

information is crucial for comprehending the potential therapeutic applications of vitexin as a potential drug for treating diseases like type 2 diabetes.

The molecular docking study reveals that epicatechin (**4**) interacts with the α-glucosidase enzyme through a variety of interactions (Fig. 7C). The interactions are mediated by the amino acids Glu271, Arg643, Tyr636, Leu640, Glu767, and Ile734. The interaction between epicatechin (**4**) and Glu271 is a Pi-Anion type interaction. Arg643 and Tyr636 form Alkyl interactions with epicatechin (**4**). Epicatechin (**4**) interacts with Leu640 through Pi-Alkyl interactions. Glu767 and Ile734 interact with epicatechin through Conventional Hydrogen Bonds. These interactions contribute to the binding of epicatechin (**4**) to the α-glucosidase enzyme. The docking analysis indicates that epicatechin (**4**) forms hydrogen bonds with specific amino acid residues, including Glu767 and Ile734. These interactions contribute to the stabilization of the epicatechin molecule within the active site, hindering the enzyme's ability to bind and hydrolyze carbohydrates.

Fig. 7D showcases a detailed molecular interaction map between isorhamnetin-3-o-rutinoside (**9**) and the α-glucosidase enzyme. This map highlights the different types of interactions between the ligand and the amino acid residues of the enzyme, providing insights into their binding affinity and potential inhibitory effect. Conventional hydrogen bonds are depicted by green lines. The ligand forms hydrogen bonds with Lys513, Lys534, and His645. These interactions suggest that the ligand is favorably positioned within the enzyme's active site, potentially hindering its activity. Isorhamnetin-3-O-rutinoside (**9**) exhibits unfavorable donor-donor interactions (depicted by red lines) with Arg520 and Arg283. These interactions are less favorable than hydrogen bonds and could contribute to the overall binding affinity. Fig. 7D also depicts several other types of interactions, such as van der Waals forces (green dotted lines) and Pi-Pi T-shaped interactions (pink dotted lines). These interactions are weaker than hydrogen bonds but still play a role in stabilizing the ligand-enzyme complex. The molecular docking results suggest that isorhamnetin-O-3-rutinoside (**9**) exhibits a combination of favorable and unfavorable interactions with the α-glucosidase enzyme. This complex interplay of forces could potentially influence the ligand's inhibitory effect on the enzyme's activity.

3.4. Molecular dynamics

Molecular dynamics (MD) simulations serve as a valuable tool for evaluating the stability and behavior of protein-ligand complexes under laboratory conditions. By simulating the atomic

interactions within the complex, MD simulations provide insights into protein conformational changes over time, helping to elucidate how protein movements can influence ligand binding stability. In our study, we conducted 200-nanosecond MD simulations on protein-ligand complexes to evaluate the ability of the candidate molecules to maintain stable interactions with the active sites of α-amylase and α-glucosidase enzymes. Throughout the simulation, various key parameters were extracted from the MD trajectory, such as Root Mean Square Deviation (RMSD), Root Mean Square Fluctuation (RMSF), and hydrogen bond interactions. These metrics were essential for determining the dynamic stability and flexibility of the protein-ligand complex

Root Mean Square Deviation (RMSD) is commonly used to assess the overall stability of a protein-ligand complex during molecular dynamics (MD) simulations. It measures the average deviation of the atomic positions from a reference structure, usually the starting structure, over time. If the RMSD remains low and relatively stable over time, it indicates that the protein-ligand complex maintains its structural integrity, suggesting that the ligand binding is stable and the protein does not undergo significant conformational changes (Patil et al., 2024; Siddiqui, Jahan, et al., 2023; Zehra et al., 2024).

The RMSD analysis for the α-amylase protein-ligand complexes, C1-α-amylase and C7-α-amylase, reveals consistent stability throughout the molecular dynamic simulations with minor fluctuations. For the **C1-α-amylase complex**, the RMSD values range from a minimum of 1.01 Å to a maximum of 2.12 Å, with an average of 1.64 Å (Table 3). Similarly, the **C7-α-amylase complex** shows a slightly broader range, with a minimum RMSD of 0.92 Å, a maximum of 2.20 Å, and an average RMSD of 1.78 Å. The low average RMSD values, coupled with the minimal fluctuations, suggest that both C1 and C7 form stable interactions with the active site of α-amylase, maintaining consistent structural integrity throughout the simulation. The RMSD analysis for the α-glucosidase protein-ligand complexes, C1-α-glucosidase and C9-α-glucosidase, demonstrates initial fluctuations attributed to the equilibration phase, a common occurrence as the system adjusts to stabilize the protein-ligand interactions. Following this brief phase, the RMSD values for both complexes stabilize, indicating consistent structural integrity throughout the remainder of the simulation. For the **C1-α-glucosidase complex**, the RMSD values range 1.00 -2.05 Å, with an average of 1.71 Å, reflecting a stable interaction between the ligand and the protein after the initial fluctuations. Similarly, the **C9-α-glucosidase complex** shows a range1.14-2.06 Å, with an average of 1.73 Å, suggesting comparable stability (Fig. 8). Despite the initial fluctuations, which are typical during the equilibration period, both

complexes maintain consistent RMSD values for the remainder of the simulation, indicating that the ligands remain securely bound within the active site of α-glucosidase.

Root Mean Square Fluctuation (RMSF) is a widely used parameter in molecular dynamics (MD) simulations to measure the flexibility of individual atoms or residues within a protein over time. RMSF provides insights into the dynamic behavior of specific regions of the protein, such as loops, secondary structures (α-helices, β-sheets), or binding sites. Low RMSF values indicate that the residues are relatively stable and undergo minimal fluctuations. These regions, often including the protein's core or key binding sites, tend to maintain their positions throughout the simulation, reflecting structural stability. In contrast, high RMSF values suggest greater flexibility or mobility in specific residues, typically located on the protein surface, such as loops or terminal regions, which may play roles in binding, conformational changes, or signal transduction (Chandole et al., 2024; Siddiqui, Jahan, et al., 2023; Siddiqui, Kumar, et al., 2023).

The RMSF analysis of the C1-α-amylase, C7-α-amylase, C1-α-glucosidase, and C9-α-glucosidase complexes offers valuable insights into the flexibility and stability of protein residues during the MD simulations. For the α-amylase protein, RMSF data for both the C1 and C7 complexes show minimal fluctuations in most regions, with minimum RMSF values of 0.35 Å for C1 and 0.34 Å for C7, and maximum values of 3.70 Å for C1 and 6.21 Å for C7. On average, the RMSF values are 0.76 Å for C1 and 0.85 Å for C7, demonstrating overall stability except for certain loop regions where higher RMSF values indicate increased flexibility. These loops contribute to the dynamic nature of the protein. Key interacting residues, including Trp58, Trp59, Tyr62, Gln63, His101, Gly104, Asn105, and others, display RMSF values ranging from 0.35 Å to 1.51 Å, illustrating stable interactions with both C1 and C7. This stability is crucial for maintaining consistent protein-ligand interactions at the active site of α-amylase.

Table 3 The Minimum, maximum and average values of different parameters, RMSD, RMSF, and Hydrogen Bonding of studied complexes.

	α-amylase Complex		**α-glucosidase Complex**	
	C1-α-amylase Complex	C7-α-amylase Complex	C1-α-glucosidase Complex	C9-α-glucosidase Complex

Root-mean-square deviation Å (RMSD)				
Minimum	1.01	0.92	1.00	1.14
Maximum	2.12	2.20	2.05	2.06
Average	1.64	1.78	1.71	1.73
Root-mean-square fluctuation Å (RMSF)				
Minimum	0.35	0.34	0.37	0.39
Maximum	3.70	6.21	6.28	4.38
Average	0.76	0.85	0.76	0.84
Hydrogen Bonding				
Minimum	1.0	1.0	1.0	1.0
Maximum	7.0	4.0	8.0	4.0
Average	2.6	0.8	4.6	1.6

For the α-glucosidase protein, the C1-α-glucosidase and C9-α-glucosidase complexes also exhibit similar stability patterns, with minimum RMSF values of 0.37 Å for C1 and 0.39 Å for C9. However, the maximum RMSF values differ, with 6.28 Å for C1 and 4.38 Å for C9, reflecting slightly more flexibility in the C1 complex (Fig. 8). The average RMSF values remain low, at 0.76 Å for C1 and 0.84 Å for C9, indicating that, overall, the residues exhibit limited fluctuations during the simulation. Interacting residues, including Glu114, His115, Glu279, Arg283, Ala285, Leu286, Ala509, and others, show RMSF values between 0.47 Å and 1.02 Å, suggesting stable interactions with both ligands. Overall, while the loop regions of the proteins display flexibility (as shown by the higher maximum RMSF values), the residues directly involved in the ligand-binding interactions remain stable. This contributes to the structural integrity and stability of the promising compounds and their interactions with α-amylase and α-glucosidase.

Hydrogen bond analysis is a critical aspect of MD simulations, providing insights into the strength and stability of protein-ligand interactions. Hydrogen bonds, which are non-covalent interactions, play a key role in maintaining the structural integrity of proteins. In protein-ligand

complexes, hydrogen bonds contribute significantly to binding affinity and specificity. Their formation can stabilize the ligand within the binding site, reduce conformational flexibility, and enhance the likelihood of successful binding. The number, duration, and strength of hydrogen bonds during MD simulations are often correlated with the stability of the complex. A higher number of consistent hydrogen bonds typically suggests a more stable and energetically favorable interaction between the ligand and the protein (Alhagri et al., 2024; Fayed et al., 2024; Khan et al., 2024). For the C1-α-amylase complex, the hydrogen bond count ranges from a minimum of 1 to a maximum of 7 bonds, with an average of 2.6 bonds. In contrast, the C7-α-amylase complex displays fewer hydrogen bonds, with a minimum of 1 and a maximum of 4 bonds, resulting in an average of 0.8 bonds. This lower bond count suggests a less stable interaction compared to C1. Moving to the C1-α-glucosidase complex, hydrogen bond formation is more robust, with a minimum of 1 bond and a maximum of 8 bonds, averaging 4.6 bonds throughout the simulation (Fig. 8). The higher average number of bonds indicates a strong and stable interaction between C1 and α-glucosidase. In comparison, the C9-α-glucosidase complex shows a more moderate interaction, with a minimum of 1 bond, a maximum of 4 bonds, and an average of 1.6 bonds. While this suggests some level of interaction, the lower bond count compared to C1 indicates that C9 forms fewer stable hydrogen bonds with α-glucosidase.

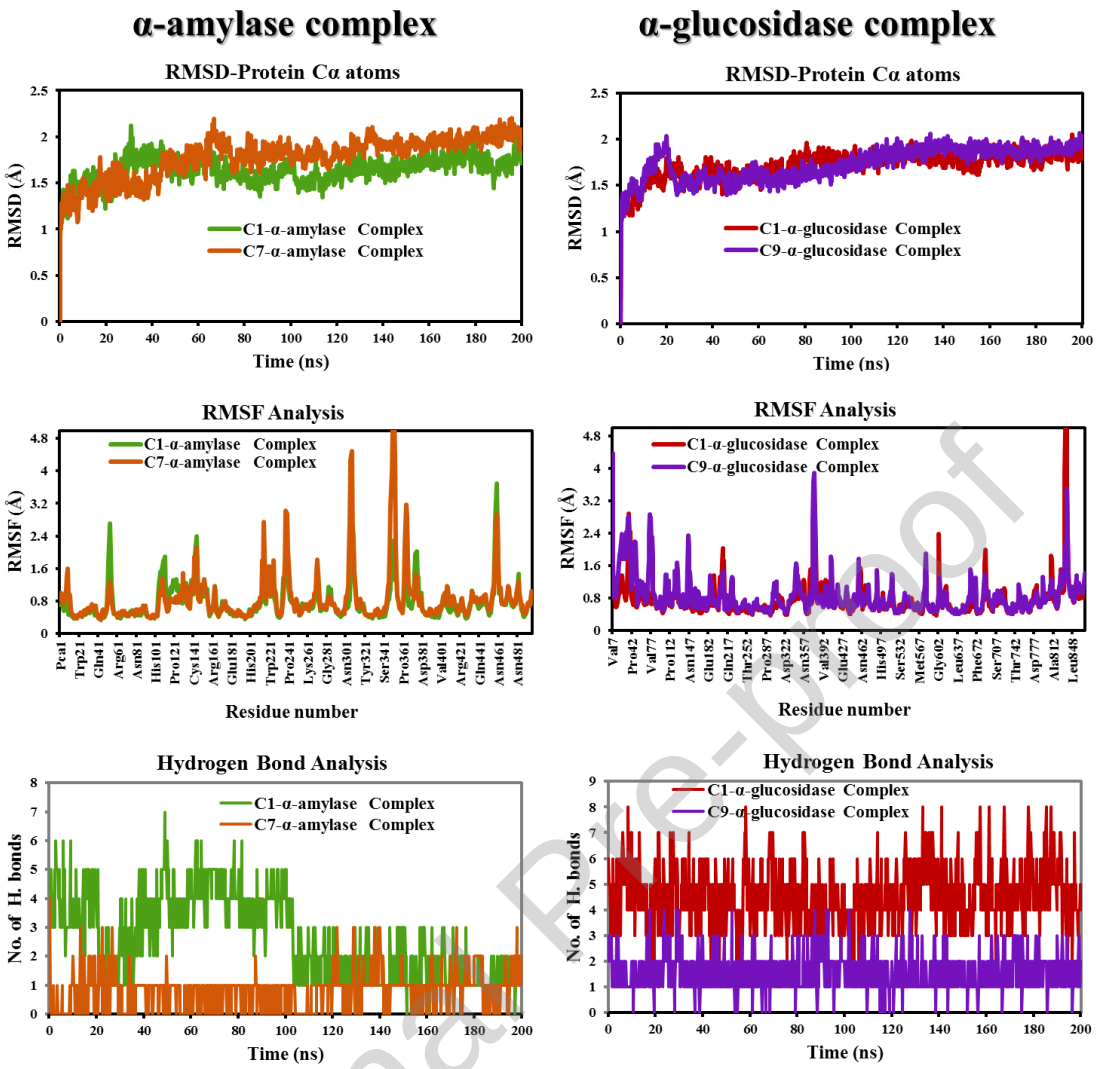

Fig. 8. Time-dependent RMSD, RMSF of individual amino acids and time-dependent Hydrogen bond analysis of α-amylase (PDB, ID: 4GQR) and α-glucosidase (PDB, ID: 2QLY) Complexes

Overall, the hydrogen bond analysis highlights that C1 consistently forms stronger and more frequent hydrogen bonds in both the α-amylase and α-glucosidase complexes, suggesting more stable and effective interactions. Meanwhile, C7 and C9 demonstrate moderate hydrogen bonding patterns, which still contribute to good stability but are less robust compared to C1.

4. Discussion

4.1. Phytochemical analysis and chemotaxonomic significance of compounds isolated from *P. thonningii*

Phytochemical analysis of the ethyl acetate extract from the leaf bark of *Piliostigma thonningii* yielded ten (1-10) known compounds, whose structures (Fig. 3) were elucidated using spectroscopic (1D and 2D NMR) and spectrometric (ESIMS) techniques, supplemented by comparison with literature data. The isolated compounds were identified as: 2H-chromen-2-one (**1**), coumarin (von Son-de Fernex et al., 2017), shikimic acid (**2**) [2], n-eicosyl-trans-ferrulate (**3**), cynnamic acid ester [3, 4], epicatechin (**4**) (Moreira-Araújo et al., 2017), genkwanin (**5**) (Ijaz et al., 2023), vitexin (**6**) (Yutharaksanukul et al., 2024), methyl β-D-glucopyranoside (**7**) (Jeffrey & Takagi, 1977), and 3,3',4',5-tetrahydroxystilbene (**8**) (INAMORI et al., 1984; Wei et al., 2024). Fractionation of the aqueous extract led to the isolation of two additional known compounds: isorhamnetin 3-O-rutinoside (**9**) (Boubaker et al., 2011; DOU et al., 2017) and kaempferol 3-O-α-L-rhamnopyranosyl-(1-2)-β-D-galactopyranoside (**10**) (Avanza et al., 2021; DOU et al., 2017; Tsiklauri et al., 2011).

Of the compounds isolated in this study, n-eicosyl-trans-ferrulate (**3**), methyl β-D-glucopyranoside (**7**), and 3,3',4',5-tetrahydroxystilbene (**8**) are newly reported from *Piliostigma thonningii*. While the antioxidant and anti-diabetic activities of most of these compounds have been reported in various other plant species, their contribution to the overall activity of *Piliostigma thonningii* had not been explored. For instance, epicatechin (**4**) is a well-known antioxidant and anti-diabetic agent (M. Afolayan et al., 2018; Nurudeen et al., 2024; Ogbiko et al., 2024). Similarly, vitexin (**6**) has been previously studied for its anti-diabetic properties, including α-amylase inhibition. This study provides the first evidence for the presence of these compounds in this specific plant species. Notably, the flavonoid compounds, including the newly identified isorhamnetin 3-O-rutinoside (**9**) and kaempferol 3-O-α-L-rhamnopyranosyl-(1-2)-β-D-galactopyranoside (**10**), along with genkwanin (**5**) and vitexin (**6**), are identified here for the first time in *Piliostigma thonningii*. These findings support the chemotaxonomic relevance of *Piliostigma thonningii*, given the widespread distribution of these compounds in plant species, including previous reports of methylflavonol, flavonol, and flavan-3-ol in *Piliostigma thonningii* (M. Afolayan et al., 2018; Nurudeen et al., 2024; Ogbiko et al., 2024) and *Piliostigma reticulatum* (Babajide et al., 2008; Boualam et al., 2021).

4.2. Antioxidant properties of *P. thonningii's* crude extracts and isolated compounds

Antioxidants possess the capacity to neutralize harmful free radicals, thereby mitigating cellular damage and reducing the risk of various diseases (Popoola et al., 2023; Xiong, 2010). Polyphenolic compounds, a subclass of antioxidants predominantly found in plant-based foods

such as fruits, vegetables, and teas, have been extensively documented to exhibit anti-inflammatory properties, enhance cardiovascular health, and confer protection against specific types of cancer (Hamadou et al., 2022; Himeda et al., 2022; Mamoudou, Obadias, et al., 2024; Núñez et al., 2023; Oscar Ditchou Nganso, Marthe Satchet Tchana, et al., 2020; Scalbert et al., 2005). A diet rich in polyphenols can augment antioxidant levels, supporting overall well-being.

Phytochemical analysis of the methanolic (MeOH) extract of *P. thonningii* revealed significant antioxidant activity, with an IC_{50} value of 184.00 µg/mL in the 2,2-diphenyl-1-picrylhydrazyl (DPPH) assay, indicative of a robust free radical neutralization capacity. This finding aligns with previous research on methanolic extracts from various plant species, which attributed antioxidant activity to the presence of phenolic compounds and flavonoids (A. M. Abubakar et al., 2021; Kabré et al., 2023; J. Tang et al., 2024; Wangso et al., 2022).

Among the isolated compounds, epicatechin (IC_{50} = 300.35 µg/mL) demonstrated promising antioxidant properties, consistent with existing literature (Abdulkhaleq et al., 2017; Moreira-Araújo et al., 2017). The flavonoids genkwanin and vitexin further underscored the role of flavonoids in enhancing antioxidant capacity, as previously reported (Abdulai et al., 2021; Chen et al., 2024; Ganesan et al., 2020; Nganso Ditchou et al., 2020).

The 2,2'-azino-bis (3-ethylbenzothiazoline-6-sulfonic acid) (ABTS) assay results corroborated the DPPH findings, with similar trends observed across extracts and compounds. Notably, the IC_{50} values for the MeOH extract (181.05 µg/mL) and EtOAc extract (197.11 µg/mL) validated the antioxidant potential of these extracts. The observed % inhibition values across all assays suggest significant and comparable antioxidant activities relative to standard antioxidants like butylated hydroxytoluene (BHT).

The free radical scavenging capacity of *P. thonningii* extracts positions them as potential natural preservatives in the food industry and therapeutic agents for managing oxidative stress-related conditions. The variation in antioxidant activity among extracts and compounds highlights the importance of phytochemical composition and extraction methods in maximizing bioactive potential.

The antioxidant activities demonstrated by *P. thonningii* extracts and isolated compounds contribute to the growing evidence supporting the health benefits of natural products and

provide a foundation for further research into their mechanisms of action and potential applications in nutraceuticals and pharmaceuticals.

4.3. *P. thonningii's* bioactive compounds as α-amylase and α-glucosidase inhibitors

The antidiabetic activities of *P. thonningii* crude extracts and their isolated compounds, as presented in the provided data, highlight significant potential for therapeutic applications in managing diabetes mellitus. The results indicate varying degrees of inhibition of α-amylase and α-glucosidase (Nganso Ditchou et al., 2024; Nnemolisa et al., 2024), two key enzymes involved in carbohydrate metabolism, which play crucial roles in postprandial glucose regulation.

Endogenous free radicals have been identified as a potential contributor to the development of Type 2 Diabetes Mellitus (T2DM). The disruption of insulin-mediated intracellular signaling pathways caused by oxidative stress has been linked to insulin resistance in individuals with excess body weight (Nurudeen et al., 2024; Scalbert et al., 2005; Shankar & Mehendale, 2014; Yutharaksanukul et al., 2024). Phenolic compounds are significant antioxidants that exert their function through various mechanisms, including the donation of a hydrogen atom to free radicals, the scavenging of other reactive species, and the binding to transition metal ions, particularly iron and copper (Abdulkhaleq et al., 2017; Huang et al., 2005; Ramatsetse et al., 2023).

The crude extracts and isolated compounds of *P. thonningii* exhibit substantial antidiabetic potential, as evidenced by their significant inhibition of α-amylase and α-glucosidase enzymes, crucial regulators of carbohydrate metabolism and postprandial glucose levels. Notably, the IC_{50} values of these extracts and compounds demonstrate robust inhibitory effects, with the MeOH extract displaying an IC_{50} of 184.45 µg/mL against α-amylase, corresponding to a 74.09% inhibition rate. This finding aligns with previous research (M. Afolayan et al., 2018; M. O. Afolayan et al., 2023; Ogbiko et al., 2024) and suggests a plausible mechanism for *P. thonningii* mediated reduction of postprandial blood glucose.

The isolated compounds, including shikimic acid and genkwanin, exhibit considerable inhibitory activities against α-glucosidase, with IC_{50} values ranging from 186.31 to 400.51 µg/mL. This is consistent with literature reports highlighting the antidiabetic properties of flavonoids and phenolic compounds, attributed to their carbohydrate-hydrolyzing enzyme inhibition (I. B. Abubakar et al., 2024; Ganesan et al., 2020; Ogbiko et al., 2024;

Yutharaksanukul et al., 2024; Zongo et al., 2023). The presence of these bioactive compounds in *P. thonningii* supports its potential as a natural source of antidiabetic agents.

4.4. Computation investigations: insight molecular mechanism of *P. thonningii's* compounds antidiabetic properties

The findings from this molecular docking study highlight several promising candidates for further investigation as potential inhibitors of α-amylase and α-glucosidase. The strong binding affinities of vitexin (**6**) and epicatechin (**4**) suggest they could be developed into therapeutic agents for managing postprandial hyperglycemia.

The current molecular docking results indicate that vitexin (**6**) and epicatechin (**4**) are promising candidates as inhibitors of α-amylase and α-glucosidase, potentially offering therapeutic benefits in managing diabetes. Their strong binding affinities align with existing literature that supports the efficacy of flavonoids in inhibiting these enzymes.

Indeed, vitexin (**6**) (-8.6 kcal/mol for α-amylase and -8.5 kcal/mol for α-glucosidase) and Epicatechin (**4**) (-8.3 kcal/mol for α-amylase and -8.2 kcal/mol for α-glucosidase) show strong binding affinities. Previous studies have reported that flavonoids (Hamadou et al., 2022; Kabré et al., 2023; Mamoudou, Obadias, et al., 2024), including vitexin and epicatechin, possess significant inhibitory effects on carbohydrate-hydrolyzing enzymes. For instance, these compounds has been documented to inhibit α-glucosidase effectively (Abdulai et al., 2021; Ganesan et al., 2020), aligning with the current findings. Vitexin has been demonstrated to restore pancreatic β-cell function and insulin signaling through the Nrf2 and NF-κB signaling pathways (Ganesan et al., 2020). Moreover, vitexin has been demonstrated to suppress the expression of adhesion molecules in endothelial cells that are upregulated by high glucose levels. This occurs through the inhibition of the NF-κB signaling pathway (Chen et al., 2024).

In addition, genkwanin (**5**) (-8.5 kcal/mol for α-glucosidase) and n-eicosyl trans ferulate (-6.1 kcal/mol) show moderate to strong binding. Genkwanin has been reported to have wide pharmacological properties (El Menyiy et al., 2023). *In vitro* and *in vivo* biological and pharmacological studies have demonstrated that genkwanin exhibits notable antioxidant and anti-inflammatory properties (El Menyiy et al., 2023; Ijaz et al., 2023; D. Tang et al., 2014). Genkwanin has been demonstrated to activate glucokinase, thereby exhibiting antihyperglycemic activity. This suggests a potential role for the compound in combating

metabolic syndrome and diabetes (El Menyiy et al., 2023; Ijaz et al., 2023; Mamoudou & Mune Mune, 2024; D. Tang et al., 2014). Furthermore, it has been demonstrated to possess cardioprotective and neuroprotective characteristics, thereby reducing the likelihood of developing cardiovascular disease and assisting in the management of neurodegenerative disorders (El Menyiy et al., 2023; Ijaz et al., 2023; D. Tang et al., 2014). Additionally, genkwanin has been demonstrated to possess additional biological properties, including anti-tumor, antibacterial, antiviral and dermo-protective effects (Bayang et al., 2025; El Menyiy et al., 2023; Ijaz et al., 2023; Leutcha et al., 2025; Mamoudou & Mune Mune, 2024; Nandwa et al., 2024; D. Tang et al., 2014).

Acarbose is a well-established α-glucosidase inhibitor used clinically to manage diabetes (Himeda et al., 2022; Nganso Ditchou et al., 2024; Nnemolisa et al., 2024). The binding affinities of the newly identified ligands suggest that they may offer comparable or superior inhibition, particularly vitexin and epicatechin.

In contrast, other ligands with moderate affinities may require additional studies to fully understand their potential and mechanisms of action. Overall, these findings contribute to the growing body of evidence supporting the use of natural compounds in metabolic disease management. The implications of these findings are profound, as they not only support the traditional use of *Piliostigma thonningii* in diabetes management but also pave the way for the development of novel antidiabetic agents based on these natural compounds. The results highlight the potential of natural compounds, particularly flavonoids, in drug development. This aligns with the growing interest in phytochemicals as sources of new drugs, emphasizing the need for further exploration of plant-derived compounds in metabolic disease management (Bayang et al., 2025; El Menyiy et al., 2023; Hamadou et al., 2022; Ijaz et al., 2023; Jagannath et al., 2025; Leutcha et al., 2025; Mamoudou & Mune Mune, 2024; Nandwa et al., 2024; D. Tang et al., 2014).

In silico protein-ligand interaction studies provide valuable mechanistic insights but are intrinsically limited. Molecular docking treats the receptor as a rigid scaffold, neglecting ligand-induced conformational adjustments, and its scoring functions approximate binding free energy without fully accounting for solvent effects or entropic contributions. Molecular dynamics simulations mitigate some of these shortcomings but remain constrained by the accuracy of the employed force fields, the finite length of the trajectories, and the fidelity of the initial crystal structure. Consequently, computational predictions may diverge from

experimental outcomes, yielding false-positive hits. Thus, hypotheses generated from docking or MD should be regarded as preliminary and require empirical validation before any claims of *in vivo* efficacy.

The key parameters from our molecular dynamics' simulations are summarized below to enhance transparency. The average Root Mean Square Deviation (RMSD) for the studied complexes was between 1.64 and 1.78 Å for α-amylase and between 1.71 and 1.73 Å for α-glucosidase. The low average RMSD values and minimal fluctuations suggest that the protein-ligand complexes exhibited stability during the 200 ns simulations. The Root Mean Square Fluctuation (RMSF) values remained low, averaging between 0.76 and 0.85 Å, with slight increases observed in loop regions, thereby affirming the overall rigidity of the active sites. The average number of hydrogen bonds, an important measure of binding stability, varied from 0.8 to 2.6 for the α-amylase complexes and from 1.6 to 4.6 for the α-glucosidase complexes. The binding free energy (ΔG) for the most stable complexes was calculated using the MM-GBSA method, yielding values of -45.21 kcal/mol for C1-α-glucosidase and -38.90 kcal/mol for C1-α-amylase. The values indicate that the binding interactions are energetically favorable and reinforce the stability observed in the MD trajectories.

Furthermore, understanding the binding interactions at a molecular level provides insights into the mechanisms by which these ligands inhibit enzyme activity. This knowledge informs the design of more potent and selective inhibitors, potentially leading to improved therapeutic outcomes. In addition, the comparison of these ligands with acarbose, a well-established drug, suggests that some of the newly identified compounds may offer comparable or superior efficacy. This could lead to the development of new treatments that may have fewer side effects or improved pharmacokinetic profiles.

4.5. Correlation between *in vitro* anti-diabetic activity and *in silico* binding affinities

An important question in natural product discovery is whether computational predictions of protein–ligand interactions truly anticipate biological activity. In this study, we compared docking-derived binding energies with experimental IC_{50} values for α-amylase and α-glucosidase inhibitors isolated from *Piliostigma thonningii*. While perfect alignment was not expected, several encouraging patterns emerged.

For α-amylase, the ordering of compounds by docking score (genkwanin > n-eicosyl trans-ferulate > shikimic acid) was identical to their inhibitory potencies *in vitro*, yielding a perfect rank correlation (Spearman ρ = 1.0). This agreement suggests that, at least for this enzyme, the docking protocol captured the key interactions governing inhibition. In contrast, the α-glucosidase data revealed only partial concordance. Genkwanin, which docked strongly (−8.1 kcal/mol), was also the most potent inhibitor experimentally (IC_{50} = 174.95 μg·mL^{-1}), comparable to the standard acarbose. Epicatechin, however, produced a slightly more favorable docking score (−8.2 kcal/mol) yet was weaker *in vitro*, while shikimic acid ranked consistently low by both metrics. This mixed outcome reflects a common reality in structure–activity studies: docking provides a qualitative filter rather than a quantitative predictor.

Table 4 Comparative ranking of *Piliostigma thonningii* compounds against α-amylase and α-glucosidase: correlation between docking affinities and *in vitro* IC_{50} values

Target	Compound	Docking (kcal/mol)	IC_{50} (μg·mL^{-1})	Rank by Dock	Rank by IC_{50}
α-amylase	Genkwanin (**5**)	−8.5	180.95	1	1
	n-Eicosyl trans-ferulate (**3**)	−6.2	202.91	2	2
	Shikimic acid (**2**)	−5.5	307.91	3	3
α-glucosidase	Genkwanin (**5**)	−8.1	174.95	2	1
	Epicatechin (**4**)	−8.2	201.51	1	3
	Shikimic acid (**2**)	−6.5	196.25	3	2
Reference	Acarbose	−7.0 / −7.0	176.51 / 171.15	—	—

The divergence between *in silico* and *in vitro* results can be rationalized by several well-known limitations. Docking estimates binding free energy under simplified conditions, often treating the receptor as rigid and ignoring solvent reorganization and entropic penalties (Hamadou et al., 2025; Pandit et al., 2025). By contrast, enzymatic inhibition in solution is influenced by solubility, compound stability, aggregation tendencies, and access to dynamic binding subsites. Furthermore, our IC_{50} values were expressed in mass units (μg·mL^{-1}), which can obscure direct comparisons across chemically diverse molecules with different molecular weights (Mamoudou, Harouna, et al., 2025; Nganso Ditchou et al., 2024; Tiwari et al., 2023). Converting to molar concentrations or deriving Ki values from kinetic analyses would sharpen the comparison.

Despite these caveats, the overall picture is consistent: compounds predicted to bind most favorably, particularly genkwanin, vitexin, and epicatechin, also emerged among the strongest inhibitors experimentally. This convergence underscores the value of docking as a triage tool, enabling efficient prioritization of phytochemicals for biochemical testing. Importantly, the

observation that genkwanin aligned across both computational and experimental platforms strengthens confidence in its candidacy as a lead antidiabetic scaffold.

Moving forward, several refinements could strengthen the link between predicted and observed activity. Experimentally, kinetic assays to derive mechanism-specific inhibition constants (Ki), alongside orthogonal biophysical techniques such as ITC, SPR, or thermal shift assays, would provide direct measures of binding affinity. Finally, *in vivo* studies addressing bioavailability and metabolic stability are crucial to establish the translational potential of these compounds.

While docking and inhibition assays are not expected to correlate perfectly, the consistency observed for genkwanin and the qualitative agreement for other flavonoids demonstrate that our *in silico* models captured essential features of enzyme inhibition. This integrative approach reinforces the therapeutic promise of *P. thonningii* flavonoids and provides a strong rationale for advancing the most active candidates into more detailed pharmacological evaluation (Mamoudou & Mune, 2025).

4.6. Study limitations and future perspectives

This study combines *in vitro* enzymatic assays with *in silico* analysis (molecular docking and dynamics simulations), providing preliminary evidence that secondary metabolites of *Piliostigma thonningii* exhibit significant antioxidant and anti-diabetic activities. However, the conclusions are limited by several intrinsic constraints of the experimental design. The dependence on isolated enzyme systems and computational models, although essential for swift screening and mechanistic understanding, fails to replicate the complete physiological environment of a living organism. As a result, essential pharmacokinetic parameters such as oral bioavailability, intestinal absorption, systemic distribution, metabolic stability, and excretion are not yet established for the phytochemicals evaluated. A compound demonstrating significant inhibition *in vitro* may undergo extensive metabolism or exhibit poor absorption *in vivo*, consequently diminishing its therapeutic significance. The current study does not examine the systemic efficacy of these agents, including their interactions with ancillary signaling cascades, potential off-target effects, or synergistic or antagonistic relationships with endogenous pathways.

To address this translational gap, future studies should focus on cellular models that accurately reflect the pathophysiology of type 2 diabetes. Experiments utilizing insulin-responsive cell

lines, such as L6 myotubes, 3T3-L1 adipocytes, or HepG2 hepatocytes, may clarify the effects of isolated constituents on glucose uptake, GLUT-4 translocation, and subsequent insulin-signaling pathways. Concurrent *in vivo* studies utilizing established rodent models of diet-induced or genetically predisposed diabetes are essential for validating the antioxidant and glycemic-modulating effects observed *in vitro*, as well as for evaluating dose–response relationships, tissue distribution, and long-term safety. Thorough toxicological profiling, encompassing acute, sub-chronic, and chronic toxicity endpoints, is crucial for identifying potential adverse pharmacodynamics that may arise at therapeutic concentrations.

This study represents a crucial initial phase, identifying several promising lead molecules and outlining a definitive roadmap for their pre-clinical development. Advancing from enzyme-centric assays to cell-based and whole-organism evaluations will enable future research to substantiate the therapeutic potential of *P. thonningii* phytochemicals and establish a foundation for clinical translation.

4.7. The potential for synergistic effects in the crude extract

Piliostigma thonningii is employed in ethnopharmacology as a complex decoction or infusion. Research indicates that the crude methanolic extract is more effective than specific flavonoids such as genkwanin and vitexin in inhibiting α-amylase and α-glucosidase. This indicates that the pharmacological effects of numerous therapeutic plants arise from various phytochemicals rather than a singular "magic bullet." Various non-exclusive pathways can interact synergistically. The combined or enhancing effect of various constituents on a common target or nodes within the carbohydrate-digestion cascade may lead to an overall inhibition that exceeds the total of the individual components (Adrien et al., 2024; Hamadou et al., 2020; Oscar Ditchou Nganso, Sidjui Sidjui, et al., 2020). The extract comprises flavonoids, tannins, and phenolic acids, which are beneficial for interactions with α-glucosidase and α-amylase, as well as for scavenging reactive oxygen species (Chiș et al., 2023; Mune Mune et al., 2024; Núñez et al., 2023). The extract mitigates post-prandial hyperglycemia and oxidative stress, factors that may contribute to the onset of diabetes. Minor components enhance the physicochemical stability and intestinal absorption of active metabolites in plant matrices, where sugar-derived glycosides facilitate the solubilization of lipophilic aglycones (Aissatou et al., 2025; Mamoudou & Mune, 2025; Núñez et al., 2023; Xia et al., 2014). Innocuous or protective molecules can reduce significant bioactive side effects, thereby broadening the therapeutic window. The antioxidant capacity of crude preparations is comparable to the synthetic standard butylated

hydroxytoluene, indicating a collaborative mechanism for radical scavenging and enzyme inhibition. The findings elucidate the historical application of *P. thonningii* in diabetes management and highlight the necessity of maintaining phytochemical integrity in both pre-clinical and clinical trials.

4.8. Structure-Activity Relationship (SAR) of isolated flavonoids

The varying inhibitory potencies of the isolated flavonoids can be explained through a structure-activity relationship (SAR) analysis, which identifies three key structural determinants. Glycosylation significantly influences bioavailability and target engagement. Glycosylated derivatives, including isorhamnetin 3 O rutinoside and kaempferol-3-O-α-L-rhamnopyranosyl-(1-2)-β-D-galactopyranoside, exhibit modified solubility and membrane permeability. Additionally, the large sugar substituents create steric constraints that may reduce binding within the enzyme's active site. The high *in-silico* affinity of isorhamnetin-3-O-rutinoside (−9.1 kcal/mol) contrasts with its moderate *in-vitro* IC_{50}, likely due to steric hindrance in solution. The pattern of hydroxylation and methylation on the flavonoid core influences antioxidant capacity and enzyme inhibition. Multiple hydroxyl groups, as seen in epicatechin and genkwanin, enhance hydrogen-bonding interactions. In contrast, methylation, such as the 7-O-methyl group in genkwanin, alters polarity and facilitates hydrophobic interactions with critical residues. Third, subtle differences between flavone and flavonol scaffolds, primarily the presence of a C2-C3 double bond and a C3 hydroxyl in flavonols, impact conformational flexibility and hydrogen-bond donor capacity; however, both subclasses significantly contribute to enzyme inhibition in this study.

The SAR insights collectively indicate that strategic alterations in glycosylation, hydroxylation, and methylation patterns can be utilized to enhance flavonoid-based inhibitors for diabetes treatment.

Conclusion

This comprehensive study provides definitive proof that *Piliostigma thonningii*-derived compounds can effectively inhibit α-amylase and α-glucosidase, the key enzymes in carbohydrate metabolism linked to type 2 diabetes. The methanolic extract demonstrated significant antioxidant activity, comparable to that of the synthetic antioxidant BHT. This proves that it is a rich source of natural antioxidants. The isolated compounds, in particular the kaempferol derivatives and methyl β-D-glucopyranoside, demonstrated unquestionable

antioxidant activity, with highly significant IC_{50} values in the DPPH and FRAP assays. Additionally, vitexin was identified as a highly potent dual inhibitor of α-amylase and α-glucosidase, with strong binding affinities observed in molecular docking studies. These results clearly demonstrate that the compounds isolated from *P. thonningii* can help mitigate postprandial hyperglycemia, which is a critical factor in the management of type 2 diabetes mellitus. The *in vitro* antioxidant and enzyme inhibitory activities, combined with *in silico* predictions of binding affinities and stabilities, provide irrefutable evidence that *P. thonningii* should be considered as a candidate for further pharmacological development. Further work must validate these results *in vivo* and evaluate the clinical relevance and safety of these compounds. *P. thonningii* is a promising natural alternative for diabetes management, offering a dual action of antioxidant and enzyme inhibitory effects and reducing reliance on synthetic drugs and their associated side effects.

CRediT authorship contribution statement

Alfred Sisinvou: Investigation, Methodology, Writing - original draft, Writing - review & editing. **Honore Wangso**: Conceptualization, Methodology, Visualization, Writing - original draft, Writing - review & editing. **Hamadou Mamoudou**: Investigation, Methodology, Data curation; Formal analysis, Methodology, Software, Writing - original draft, Writing - review & editing. **Sali Mouhamadou**: Investigation, Data curation; Formal analysis, Methodology, Software, Writing - original draft. **Bargui Benoit Koubala**: Conceptualization, Investigation, Methodology, Supervision, Validation, Visualization, Writing - original draft, Writing - review & editing. **Prof. Perwez Alam:** Methodology, Visualization, Writing - original draft, Writing - review & editing. **Sophie Laurent**: Investigation, Data curation; Formal analysis, Methodology, Writing – review original draft. **Celine Henoumont**: Investigation, Data curation; Formal analysis, Methodology, Writing – review original draft. **Mohit Agrawal:** Methodology, Visualization, Writing - original draft, Writing - review & editing. **Emmanuel Talla**: Conceptualization, Investigation, Methodology, Supervision, Validation, Visualization, Writing - original draft, Writing - review & editing.

Disclosure statement

No conflict of interest.

Acknowledgements

The authors are indebted to the Department of General, Organic Chemistry and Biomedical, Laboratory of NMR and molecular Imaging of the University of Mons, Belgium. The authors gratefully acknowledge the technical support and resources provided by the Laboratory of Biochemistry and Biological Chemistry of the University of Maroua, Cameroon. Additionally, Prof. Mohamed F AlAjmi wishes to express his appreciation for the financial support received from the Researchers Supporting Project (RSP 2025R122), King Saud University, Riyadh, Saudi Arabia.

Funding

No funding supported this research investigation.

References

Abdulai, I. L., Kwofie, S. K., Gbewonyo, W. S., Boison, D., Puplampu, J. B., & Adinortey, M. B. (2021). Multitargeted Effects of Vitexin and Isovitexin on Diabetes Mellitus and Its Complications. *The Scientific World Journal*, *2021*, 1–20. https://doi.org/10.1155/2021/6641128

Abdulkhaleq, L. A., Assi, M. A., Noor, M. H. M., Abdullah, R., Saad, M. Z., & Taufiq-Yap, Y. H. (2017). Therapeutic uses of epicatechin in diabetes and cancer. *Veterinary World*, *10*(8), 869–872. https://doi.org/10.14202/vetworld.2017.869-872

Abubakar, A. M., Soltanifar, Z., Luka, Y., Udoh, E. W., & Hamadou, M. (2021). Analysis of Microbial Growth Models for Microorganisms in Chicken Manure Digester. *International Journal of Research In Science & Engineering*, *12*, 1–24. https://doi.org/10.55529/ijrise.12.1.24

Abubakar, I. B., Malami, I., Muhammad, A., Salihu Shinkafi, T., Shehu, D., & Maduabuchi Aja, P. (2024). A review of the medicinal uses and biological activity of Piliostigma thonningii (Schum). Milne-Redh. *RPS Pharmacy and Pharmacology Reports*, *3*(1). https://doi.org/10.1093/rpsppr/rqae004

Adewole, T. S., Bieni, M. C., Ogundepo, G. E., Odekanyin, O. O., & Kuku, A. (2024). Investigation of functional, antioxidant, anti-inflammatory, and antidiabetic properties of legume seed protein hydrolysates. *Food Hydrocolloids for Health*, *5*, 100175. https://doi.org/10.1016/j.fhfh.2023.100175

Adrien, L. T., Kidjama, N. N., Didier, B., Germain, T. S., Madi, H., & Elisabeth, N. B. (2024).

Acute and Sub-acute Oral Toxicity Studies of an Aqueous Extract of Ocimum gratissimum (Lamiaceae) in the Mouse Mus Musculus. *Journal of Advances in Medical and Pharmaceutical Sciences*, *26*(9), 17–34. https://doi.org/10.9734/jamps/2024/v26i9711

Afolayan, M. O., Omosimua, R. O., Fadeyi, A. E., Aguzue, O. C., Asekun, O. T., & Familoni, O. B. (2023). *Phytochemical, Antioxidant, and Flavonoid Investigation of Methanolic Leaf Extract of Piliostigma thonningii (Schum.)* (pp. 1–26). https://doi.org/10.1007/978-1-0716-2683-2_1

Afolayan, M., Srivedavyasasri, R., Asekun, O. T., Familoni, O. B., Orishadipe, A., Zulfiqar, F., Ibrahim, M. A., & Ross, S. A. (2018). Phytochemical study of Piliostigma thonningii, a medicinal plant grown in Nigeria. *Medicinal Chemistry Research*, *27*(10), 2325–2330. https://doi.org/10.1007/s00044-018-2238-1

Aissatou, Aboubakar, Hamadou, M., & Abdoulaye, M. (2025). Novel formulation of black garlic and sesame seeds (Sesamum indicum): evaluating antioxidant and antihyperlipidemic effects through in vitro and in vivo models. *Food Chemistry Advances*, *8*, 101089. https://doi.org/10.1016/j.focha.2025.101089

Alhagri, I. A., Alsowayan, R., Ghannay, S., Al-Hazmy, S. M., Ahmad, I., Patel, H., Kadri, A., & Aouadi, K. (2024). Synthesis, optical properties, DNA, β-cyclodextrin interactions, and antioxidant evaluation of novel isoxazolidine derivative (ISoXD2): A multispectral and computational analysis. *Heliyon*, *10*(14), e34561. https://doi.org/10.1016/j.heliyon.2024.e34561

Amang à Ngnoung, G. A., Nganso Ditchou, Y. O., Leutcha, P. B., Dize, D., Tatsimo, S. J. N., Tchokouaha, L. R. Y., Kowa, T. K., Tembeni, B., Mamoudou, H., Poka, M., Demana, P. H., Siwe Noundou, X., Fekam Boyom, F., & Meli Lannang, A. (2023). Antiplasmodial and Antileishmanial Activities of a New Limonoid and Other Constituents from the Stem Bark of Khaya senegalensis. *Molecules*, *28*(20), 7227. https://doi.org/10.3390/molecules28207227

Avanza, M. V., Álvarez-Rivera, G., Cifuentes, A., Mendiola, J. A., & Ibáñez, E. (2021). Phytochemical and Functional Characterization of Phenolic Compounds from Cowpea (Vigna unguiculata (L.) Walp.) Obtained by Green Extraction Technologies. *Agronomy*, *11*(1), 162. https://doi.org/10.3390/agronomy11010162

Babajide, O. J., Babajide, O. O., Daramola, A. O., & Mabusela, W. T. (2008). Flavonols and an oxychromonol from Piliostigma reticulatum. *Phytochemistry*, *69*(11), 2245–2250. https://doi.org/10.1016/j.phytochem.2008.05.003

Bayang, J. P., Touwang, C., Mamoudou, H., Woudam, E. S., & Koubala, B. B. (2025).

Variation of nutrients and bioactive compounds of five wild edible leafy vegetables from far north region of cameroon. *Food Chemistry Advances*, *6*, 100849. https://doi.org/10.1016/j.focha.2024.100849

Benzie, I. F. F., & Strain, J. J. (1996). The Ferric Reducing Ability of Plasma (FRAP) as a Measure of "Antioxidant Power": The FRAP Assay. *Analytical Biochemistry*, *239*(1), 70–76. https://doi.org/10.1006/ABIO.1996.0292

Bochkov, D. V, Sysolyatin, S. V, Kalashnikov, A. I., & Surmacheva, I. A. (2012). Shikimic acid: review of its analytical, isolation, and purification techniques from plant and microbial sources. *Journal of Chemical Biology*, *5*(1), 5–17. https://doi.org/10.1007/s12154-011-0064-8

Boualam, K., Ndiaye, B., Harhar, H., Tabyaoui, M., Ayessou, N., & Taghzouti, K. (2021). Study of the Phytochemical Composition, the Antioxidant and the Anti-Inflammatory Effects of Two Sub-Saharan Plants: Piliostigma reticulatum and Piliostigma thonningii. *Advances in Pharmacological and Pharmaceutical Sciences*, *2021*, 1–8. https://doi.org/10.1155/2021/5549478

Boubaker, J., Bhouri, W., Ben Sghaier, M., Ghedira, K., Dijoux Franca, M. G., & Chekir-Ghedira, L. (2011). Ethyl acetate extract and its major constituent, isorhamnetin 3-O-rutinoside, from Nitraria retusa leaves, promote apoptosis of human myelogenous erythroleukaemia cells. *Cell Proliferation*, *44*(5), 453–461. https://doi.org/10.1111/j.1365-2184.2011.00772.x

Brayer, G. D., Luo, Y., & Withers, S. G. (1995). The structure of human pancreatic α -amylase at 1.8 Å resolution and comparisons with related enzymes. *Protein Science*, *4*(9), 1730–1742. https://doi.org/10.1002/pro.5560040908

Chandole, P. K., Pawar, T. J., Olivares-Romero, J. L., Tivari, S. R., Garcia Lara, B., Patel, H., Ahmad, I., Delgado-Alvarado, E., Kokate, S. V., & Jadeja, Y. (2024). Exploration of novel cationic amino acid-enriched short peptides: design, SPPS, biological evaluation and in silico study. *RSC Advances*, *14*(25), 17710–17723. https://doi.org/10.1039/D3RA08313F

Chang, S.-J., Lin, T.-H., & Chen, C.-C. (2001). CONSTITUENTS FROM THE STEMS OF DENDROBIUM CLAVATUM VAR. AURANTIACUM. *J Chin Med*, *12*(3), 211–218.

Chen, P.-C., Chang, Y.-C., Tsai, K.-L., Shen, C. H., & Lee, S.-D. (2024). Vitexin Suppresses High-Glucose-upregulated Adhesion Molecule Expression in Endothelial Cells through Inhibiting NF-κB Signaling Pathway. *ACS Omega*. https://doi.org/10.1021/acsomega.4c02545

Chiș, A., Noubissi, P. A., Pop, O.-L., Mureșan, C. I., Fokam Tagne, M. A., Kamgang, R., Fodor,

A., Sitar-Tăut, A.-V., Cozma, A., Orășan, O. H., Hegheș, S. C., Vulturar, R., & Suharoschi, R. (2023). Bioactive Compounds in Moringa oleifera: Mechanisms of Action, Focus on Their Anti-Inflammatory Properties. *Plants*, *13*(1), 20. https://doi.org/10.3390/plants13010020

DOU, L.-L., DUAN, L., GUO, L., LIU, L.-L., ZHANG, Y.-D., LI, P., & LIU, E.-H. (2017). An UHPLC-MS/MS method for simultaneous determination of quercetin 3- O -rutinoside, kaempferol 3- O -rutinoside, isorhamnetin 3- O -rutinoside, bilobalide and ligustrazine in rat plasma, and its application to pharmacokinetic study of Xingxiong injection. *Chinese Journal of Natural Medicines*, *15*(9), 710–720. https://doi.org/10.1016/S1875-5364(17)30101-2

El Menyiy, N., Aboulaghras, S., Bakrim, S., Moubachir, R., Taha, D., Khalid, A., Abdalla, A. N., Algarni, A. S., Hermansyah, A., Ming, L. C., Rusu, M. E., & Bouyahya, A. (2023). Genkwanin: An emerging natural compound with multifaceted pharmacological effects. *Biomedicine & Pharmacotherapy*, *165*, 115159. https://doi.org/10.1016/j.biopha.2023.115159

Fayed, M. A. A., Abdallah, I. A., Ahmad, I., Patel, H., & Abdou, E. M. (2024). Green nanotechnology for targeted drug delivery: UPLC-ESI-MS/MS, In vitro/ In silico Cytotoxic and Antibacterial Activity of Pimpinella anisum L. and Its Silver Nanoparticles. *Journal of Molecular Structure*, *1314*, 138800. https://doi.org/10.1016/j.molstruc.2024.138800

Ganesan, K., Ramkumar, K. M., & Xu, B. (2020). Vitexin restores pancreatic β-cell function and insulin signaling through Nrf2 and NF-κB signaling pathways. *European Journal of Pharmacology*, *888*, 173606. https://doi.org/10.1016/j.ejphar.2020.173606

Gao, C., Wang, F., Yuan, L., Liu, J., Sun, D., & Li, X. (2019). Physicochemical property, antioxidant activity, and cytoprotective effect of the germinated soybean proteins. *Food Science & Nutrition*, *7*(1), 120–131. https://doi.org/10.1002/FSN3.822

Hailemariam, M. B., Woldu, Z., Asfaw, Z., & Lulekal, E. (2021). Ethnobotany of an indigenous tree Piliostigma thonningii (Schumach.) Milne-Redh. (Fabaceae) in the arid and semi-arid areas of South Omo Zone, southern Ethiopia. *Journal of Ethnobiology and Ethnomedicine*, *17*(1), 44. https://doi.org/10.1186/s13002-021-00469-6

Hamadou, M., Daoudou, B., Paul, B. M.-, Mohamadou, S., & Roger, D. D. (2020). Inhibitory Effect of Methanolic and Methanolic-Aqueous Mixture Extract of Leaves of Plectranthus neochilus Schltr (Lamiaceae) and Bauhinia rufescens Lam (Fabaceae) on Two Strains of Enterobacteria Producing Beta-lactamases. *Journal of Advances in Microbiology*, 11–20.

https://doi.org/10.9734/jamb/2020/v20i730259

Hamadou, M., Martin Alain, M. M., Obadias, F. V., Hashmi, M. Z., Başaran, B., Jean Paul, B., & Samuel René, M. (2022). Consumption of underutilised grain legumes and the prevention of type II diabetes and cardiometabolic diseases: Evidence from field investigation and physicochemical analyses. *Environmental Challenges*, *9*, 100621. https://doi.org/10.1016/j.envc.2022.100621

Hamadou, M., Nganso Ditchou, Y. O., Leutcha, P. B., Mujwar, S., Mune Mune, M. A., & Siwe Noundou, X. (2025). Computation drug design for ACE inhibitor for high blood pressure management and assessment of pharmacokinetics and toxicity of promising compounds isolated from Gymnema sylvestre. *Bioorganic Chemistry*, *164*, 108896. https://doi.org/10.1016/j.bioorg.2025.108896

Himeda, M., Bechir, M., Aboubakar, ., Abakoura, B., Tidjani, A., & Hamadou, M. (2022). State of Fruit and Vegetable Consumption in N'Djamena, Chad. *European Journal of Medicinal Plants*, 37–47. https://doi.org/10.9734/ejmp/2022/v33i930489

Huang, D., Ou, B., & Prior, R. L. (2005). The Chemistry behind Antioxidant Capacity Assays. *Journal of Agricultural and Food Chemistry*, *53*(6), 1841–1856. https://doi.org/10.1021/jf030723c

Ibrahim, M. A., Bester, M. J., Neitz, A. W., & Gaspar, A. R. M. (2018). Rational in silico design of novel α-glucosidase inhibitory peptides and in vitro evaluation of promising candidates. *Biomedicine & Pharmacotherapy*, *107*, 234–242. https://doi.org/10.1016/j.biopha.2018.07.163

Ijaz, M. U., Ishtiaq, A., Tahir, A., Alvi, M. A., Rafique, A., Wang, P., & Zhu, G. (2023). Antioxidant, anti-inflammatory, and anti-apoptotic effects of genkwanin against aflatoxin B1-induced testicular toxicity. *Toxicology and Applied Pharmacology*, *481*, 116750. https://doi.org/10.1016/j.taap.2023.116750

INAMORI, Y., KATO, Y., KUBO, M., YASUDA, M., BABA, K., & KOZAWA, M. (1984). Physiological activities of 3,3',4,5'-tetrahydroxystilbene isolated from the heartwood of Cassia garrettiana CRAIB. *Chemical and Pharmaceutical Bulletin*, *32*(1), 213–218. https://doi.org/10.1248/cpb.32.213

Ipe, R., Oh, J. M., Kumar, S., Ahmad, I., Nath, L. R., Bindra, S., Patel, H., Kolachi, K. Y., Prabhakaran, P., Gahtori, P., Syed, A., Elgorbanh, A. M., Kim, H., & Mathew, B. (2024). Inhibition of monoamine oxidases and neuroprotective effects: chalcones vs. chromones. *Molecular Diversity*. https://doi.org/10.1007/s11030-024-10959-w

Jagannath, S., Vinayak, W., Amol, M., Sandhya, P., V.M, C., Vaibhav, S., & Kulkarni, R.

(2025). Molecular dynamics directed neuroprotective activity of alcoholic extract of Garuga pinnata Roxb. in experimental rats. *Journal of Ayurveda and Integrative Medicine*, *16*(1), 101032. https://doi.org/10.1016/j.jaim.2024.101032

Jeffrey, G. A., & Takagi, S. (1977). The crystal and molecular structure of methyl β-D-glucopyranoside hemihydrate. *Acta Crystallographica Section B Structural Crystallography and Crystal Chemistry*, *33*(3), 738–742. https://doi.org/10.1107/S0567740877004579

Kabré, P., Ouattara, L., Sanou, Y., Ouédraogo, R. J., Ouoba, P., Zanté, A.-A., Zoungo, D., Somda, M. B., & Ouédraogo, G. A. (2023). Comparative study of polyphenols, flavonoids content, antioxidant and antidiabetic activities of Lophira lanceolata Tiegh.ex Keay (Ochnaceae) extracts. *Scientific African*, *22*, e01922. https://doi.org/10.1016/j.sciaf.2023.e01922

Khan, M., Khan, S., Alshammary, F. L., Goyal, U., Singh, V., Ahmad, I., Patel, H., Gupta, V. K., & Haque, S. (2024). Exploring the synergistic therapeutic potential of Morus alba extract in tuberculosis: A computational analysis. *Journal of King Saud University - Science*, *36*(9), 103371. https://doi.org/10.1016/j.jksus.2024.103371

Leutcha, P. B., Mamoudou, H., Nganso Ditchou, Y. O., Ansari, S. A., Amang à Ngnoung, G. A., Mujwar, S., Domga Taiga, J., Agrawal, M., Messah Nembot, G., Boubakari Hamadou, S., Meli Lannang, A., & Siwe Noundou, X. (2025). Flavonoids and other constituents from Jacaranda mimosifolia: In vitro analysis, molecular docking, and molecular dynamic simulations of antioxidant and anti-inflammatory activities. *Biomedicine & Pharmacotherapy*, *182*, 117768. https://doi.org/10.1016/j.biopha.2024.117768

Luka, Y., Highina, B. K., Zubairu, A., Adeleke, A. J., Hamadou, M., Abubakar Musti, Y., Musa Abubakar, A., & Umar Yunus, M. (2024). Biosorption as Technique for Remediation of Heavy Metals from Wastewater using Microbial Biosorbent. *Biological Sciences*, *04*(01). https://doi.org/10.55006/biolsciences.2024.4105

Mamoudou, H., Abdoulaye, A. H., Ditchou, N. Y. O., Olumasai, J. N., Adissa, R. M. Z. K., & Mune, M. A. M. (2025). Computational investigation of Plectranthus neochilus essential oil phytochemicals interaction with dipeptidyl peptidase 4: a potential avenue for antidiabetic drug discovery. *Current Pharmaceutical Analysis*, *21*(3), 169–178. https://doi.org/10.1016/j.cpan.2025.03.002

Mamoudou, H., Başaran, B., Mune, M. A. M., Abubakar, A. M., Nandwa, J. O., Raimi, M. K. Z., & Hashmi, M. Z. (2024). Bioactive peptides derived from the enzymatic hydrolysis of cowhide collagen for the potential treatment of atherosclerosis: A computational approach.

Intelligent Pharmacy, *2*(4), 456–466. https://doi.org/10.1016/j.ipha.2024.05.004

Mamoudou, H., Harouna, D. V., Nandwa, J. O., Yonas, V., & Mune, M. A. M. (2025). Aflatoxigenic Fungi and Groundnut. In *Aflatoxigenic Fungi* (pp. 94–114). CRC Press. https://doi.org/10.1201/9781003487043-15

Mamoudou, H., & Mune, M. A. M. (2025). AI-driven bioactive peptide discovery of next-generation metabolic biotherapeutics. *Applied Food Research*, 101291. https://doi.org/10.1016/j.afres.2025.101291

Mamoudou, H., & Mune Mune, M. A. (2024). Investigating Bambara bean (Vigna subterranea (Verdc.) L.) protein and hydrolysates: a comprehensive analysis of biological and biochemical properties. *Applied Food Research*, *4*(2), 100489. https://doi.org/10.1016/j.afres.2024.100489

Mamoudou, H., Obadias, F. V., Samuel René, M., & Martin Alain, M. M. (2024). Physical characteristics, chemical composition, and antioxidant properties of defatted grain legumes cultivated in Diamare division (Far North Region, Cameroon). *Applied Food Research*, *4*(2), 100498. https://doi.org/10.1016/j.afres.2024.100498

Moreira-Araújo, R. S. dos R., Sampaio, G. R., Soares, R. A. M., Silva, C. P., & Arêas, J. A. G. (2017). Identification and quantification of antioxidant compounds in cowpea1. *Revista Ciência Agronômica*, *48*(5), 799–805. https://doi.org/10.5935/1806-6690.20170093

Mouhamadou, S., Dalhatou, S., Dobe, N., Djakba, R., Fasanya, O. O., Bansod, N. D., Fita, G., Ngayam, C. H., Tejeogue, J. P. N., & Harouna, M. (2023). Linear and Non-linear Modelling of Kinetics and Equilibrium Data for Cr(VI) Adsorption by Activated Carbon Prepared from Piliostigma reticulatum. *Chemistry Africa*, *6*(2), 719–731. https://doi.org/10.1007/s42250-022-00324-5

Mouhamadou, S., Dalhatou, S., Obada, D. O., Fryda, L., Mahieu, A., Bonnet, P., Caperaa, C., Kane, A., Massai, H., & Zeghioud, H. (2023). Synthesis of piliostigma reticulatum decorated TiO2 based composite and its application towards Cr(VI) adsorption and bromophenol blue degradation: Nonlinear kinetics, equilibrium modelling and optimisation photocatalytic parameters. *Journal of Environmental Chemical Engineering*, *11*(1), 109273. https://doi.org/10.1016/j.jece.2023.109273

Mudgil, P., Al Dhaheri, M. K. O., Alsubousi, M. S. M., Khan, H., Redha, A. A., Yap, P.-G., Gan, C.-Y., & Maqsood, S. (2024). Molecular docking studies on α-amylase inhibitory peptides from milk of different farm animals. *Journal of Dairy Science*, *107*(5), 2633–2652. https://doi.org/10.3168/jds.2023-24118

Mueed, A., Shibli, S., Al-Quwaie, D. A., Ashkan, M. F., Alharbi, M., Alanazi, H., Binothman,

N., Aljadani, M., Majrashi, K. A., Huwaikem, M., Abourehab, M. A. S., Korma, S. A., & El-Saadony, M. T. (2023). Extraction, characterization of polyphenols from certain medicinal plants and evaluation of their antioxidant, antitumor, antidiabetic, antimicrobial properties, and potential use in human nutrition. *Frontiers in Nutrition*, *10*. https://doi.org/10.3389/fnut.2023.1125106

Mune Mune, M. A., Hatanaka, T., Kishimura, H., & Kumagai, Y. (2024). Understanding Antidiabetic Potential of Oligosaccharides from Red Alga Dulse Devaleraea inkyuleei Xylan by Investigating α-Amylase and α-Glucosidase Inhibition. *Molecules*, *29*(7), 1536. https://doi.org/10.3390/molecules29071536

Nandwa, J. O., Mehmood, A., Mahjabeen, I., Raheem, K. Y., Hamadou, M., Raimi, M. Z. K. A., & Kayani, M. A. (2024). miR-4716–3p and the target AKT2 Gene/rs2304186 SNP are associated with blood cancer pathogenesis in Pakistani population. *Non-Coding RNA Research*, *9*(3), 695–703. https://doi.org/10.1016/j.ncrna.2024.03.005

Nganso Ditchou, Y. O., Leutcha, P. B., Miaffo, D., Mamoudou, H., Ali, M. S., Amang à Ngnoung, G. A., Soh, D., Agrawal, M., Darbawa, R., Zondegoumba Nkwengoua Tchouboun, E., Meli Lannang, A., & Siwe Noundou, X. (2024). In vitro and in silico assessment of antidiabetic and antioxidant potencies of secondary metabolites from Gymnema sylvestre. *Biomedicine & Pharmacotherapy*, *177*, 117043. https://doi.org/10.1016/j.biopha.2024.117043

Nganso Ditchou, Y. O., Soh, D., Nkwengoua Tchouboun, E. Z., Tchana Satchet, E. M., Mamoudou, H., & Nyassé, B. (2020). Qualitative Analysis of Peptides and Biological Activities of Allexis cauliflora (Violaceae) Leaves. *Journal of Natural Products and Resources*, *6*(1), 252–257. https://doi.org/10.30799/jnpr.088.20060104

Nnemolisa, S. C., Chukwurah, C. C., Edeh, S. C., Aguchem, R. N., Chibuogwu, C. C., Aham, E. C., Chukwu, M. C., Obiora, M. O., Anyebe, D. E., & Okagu, I. U. (2024). Antidiabetic and Antioxidant Potentials of Pleurotus ostreatus -derived Compounds: An in vitro and in silico approach. *Food Chemistry Advances*, 100639. https://doi.org/10.1016/j.focha.2024.100639

Núñez, S., Moliner, C., Valero, M. S., Mustafa, A. M., Maggi, F., Gómez-Rincón, C., & López, V. (2023). Antidiabetic and anti-obesity properties of a polyphenol-rich flower extract from Tagetes erecta L. and its effects on Caenorhabditis elegans fat storages. *Journal of Physiology and Biochemistry*, *79*(2), 427–440. https://doi.org/10.1007/s13105-023-00953-5

Nurudeen, Q. O., Yusuf, Z. M., Salimon, S. S., Falana, M. B., Ayinla, A., Asinmi, M. R., Oweh,

O. T., & Dikwa, M. A. (2024). Hydroethanolic extract of Piliostigma thonningii leaves extenuates the severity of diarrhoea in female Wistar rats. *Journal of Complementary and Integrative Medicine*, *21*(1), 26–37. https://doi.org/10.1515/jcim-2023-0205

Ogbiko, C., Jonathan, E. C., Joseph, I. C., & Chiedu, O. F. B. (2024). Isolation, characterization, and screening of secondary metabolites from endophytic fungi isolated from Nigerian Piliostigma thonningii for antimicrobial activities. *Journal of Drug Delivery and Therapeutics*, *14*(6), 15–22. https://doi.org/10.22270/jddt.v14i6.6510

Oscar Ditchou Nganso, Y., Marthe Satchet Tchana, E., Doutsing Kahouo, A., Gabrielle à Ngnoung Amang, A., Abah, K., Fomena, H., & Mamoudou, H. (2020). Inhibitory Effect and Antimicrobial Activity of Secondary Metabolites of <i>Khaya Senegalensis</i> (Desr.) A. Juss. (Meliaceae). *Science Journal of Chemistry*, *8*(4), 92. https://doi.org/10.11648/j.sjc.20200804.13

Oscar Ditchou Nganso, Y., Sidjui Sidjui, L., Gabrielle A Ngnoung Amang, A., Doutsing Kahouo, A., Abah, K., Fomena, H., & Hamadou, M. (2020). Identification of Peptides in the Leaves of <i>Bauhinia rufescens</i> Lam (Fabaceae) and Evaluation of Their Antimicrobial Activities Against Pathogens for Aquaculture. *Science Journal of Chemistry*, *8*(4), 81. https://doi.org/10.11648/j.sjc.20200804.12

Pandit, G. K., Abubakar, A. M., Mamoudou, H., Tariq, M., Abdulrazak, M., Wali, S. A., & Asif, M. (2025). Molecular underpinning of plants hormonal signaling to abiotic stressors using plant chemical and synthetic biology approaches. In *Role of Antioxidants in Abiotic Stress Management* (pp. 383–393). Elsevier. https://doi.org/10.1016/B978-0-443-14139-3.00012-9

Patil, B. R., Bhadane, K. V., Ahmad, I., Agrawal, Y. J., Shimpi, A. A., Dhangar, M. S., & Patel, H. M. (2024). Exploring the structural activity relationship of the Osimertinib: A covalent inhibitor of double mutant EGFRL858R/T790M tyrosine kinase for the treatment of Non-Small Cell Lung Cancer (NSCLC). *Bioorganic & Medicinal Chemistry*, *109*, 117796. https://doi.org/10.1016/j.bmc.2024.117796

Popoola, J. O., Ojuederie, O. B., Aworunse, O. S., Adelekan, A., Oyelakin, A. S., Oyesola, O. L., Akinduti, P. A., Dahunsi, S. O., Adegboyega, T. T., Oranusi, S. U., Ayilara, M. S., & Omonhinmin, C. A. (2023). Nutritional, functional, and bioactive properties of african underutilized legumes. *Frontiers in Plant Science*, *14*, 1105364. https://doi.org/10.3389/fpls.2023.1105364

Raimi, M. Z. K. A., Nadeem, A., Raheem, K., Hussain, G., Zafeer, N., Hamadou, M., Irfan, M., Nandwa, J., Ahmad, F., Ullah, A., & Shabbir, A. (2024). In silico analysis of RPS4X (X-

linked ribosomal protein) with active components from black seed (Nigella sativa) for potential treatment of multiple sclerosis. *Journal of Molecular Structure*, *1297*, 136909. https://doi.org/10.1016/j.molstruc.2023.136909

Ramatsetse, K. E., Ramashia, S. E., & Mashau, M. E. (2023). A review on health benefits, antimicrobial and antioxidant properties of Bambara groundnut (Vigna subterranean). *International Journal of Food Properties*, *26*(1), 91–107. https://doi.org/10.1080/10942912.2022.2153864

Rathod, B., Puri, S., Juvale, K., Ansari, I., Patel, H., Baldaniya, L., & Kumar, K. (2024). Synthesis and evaluation of tryptanthrin derivatives as promising anticancer agents: In vitro, in silico, and SAR insights. *Journal of Molecular Structure*, *1311*, 138365. https://doi.org/10.1016/j.molstruc.2024.138365

Scalbert, A., Manach, C., Morand, C., Rémésy, C., Jiménez, L., Emésy, C. R. ′, Emésy, E., & Jiménez, J. (2005). Dietary polyphenols and the prevention of diseases. *Taylor & Francis*, *45*(4), 287–306. https://doi.org/10.1080/1040869059096

Shankar, K., & Mehendale, H. M. (2014). Oxidative Stress. In *Encyclopedia of Toxicology* (pp. 735–737). Elsevier. https://doi.org/10.1016/B978-0-12-386454-3.00345-6

Siddiqui, A. J., Jahan, S., Siddiqui, M. A., Khan, A., Alshahrani, M. M., Badraoui, R., & Adnan, M. (2023). Targeting Monoamine Oxidase B for the Treatment of Alzheimer's and Parkinson's Diseases Using Novel Inhibitors Identified Using an Integrated Approach of Machine Learning and Computer-Aided Drug Design. *Mathematics*, *11*(6), 1464. https://doi.org/10.3390/math11061464

Siddiqui, A. J., Jamal, A., Zafar, M., & Jahan, S. (2024). Identification of TBK1 inhibitors against breast cancer using a computational approach supported by machine learning. *Frontiers in Pharmacology*, *15*. https://doi.org/10.3389/fphar.2024.1342392

Siddiqui, A. J., Kumar, V., Jahan, S., Alshahrani, M. M., Al Awadh, A. A., Siddiqui, M. A., Hamadou, W. S., Abdelgadir, A., Saxena, J., Badraoui, R., Snoussi, M., & Adnan, M. (2023). Computational insight into structural basis of human ELOVL1 inhibition. *Computers in Biology and Medicine*, *157*, 106786. https://doi.org/10.1016/j.compbiomed.2023.106786

Su, N., Yi, L., He, J., Ming, L., Jambal, T., Mijiddorj, B., Maizul, B., Enkhtuul, T., & Ji, R. (2024). Identification and molecular docking of a novel antidiabetic peptide from protamex-camel milk protein hydrolysates against α-amylase and DPP-IV. *International Dairy Journal*, 105884. https://doi.org/10.1016/j.idairyj.2024.105884

Sun, T., Tang, J., & Powers, J. R. (2005). Effect of pectolytic enzyme preparations on the

phenolic composition and antioxidant activity of asparagus juice. *Journal of Agricultural and Food Chemistry*, *53*(1), 42–48. https://doi.org/10.1021/JF0491299

Tang, D., Yu, Y., Zheng, X., Wu, J., Li, Y., Wu, X., Du, Q., & Yin, X. (2014). Comparative investigation of in vitro biotransformation of 14 components in Ginkgo biloba extract in normal, diabetes and diabetic nephropathy rat intestinal bacteria matrix. *Journal of Pharmaceutical and Biomedical Analysis*, *100*, 1–10. https://doi.org/10.1016/j.jpba.2014.07.022

Tang, J., Li, R., Wu, B., Tang, J., Kan, H., Zhao, P., Zhang, Y., Wang, W., & Liu, Y. (2024). Secondary Metabolites with Antioxidant and Antimicrobial Activities from Camellia fascicularis. *Current Issues in Molecular Biology*, *46*(7), 6769–6782. https://doi.org/10.3390/cimb46070404

Tiwari, V. P., Dubey, A., Al-Shehri, M., & Tripathi, I. P. (2023). Exploration of human pancreatic alpha-amylase inhibitors from Physalis peruviana for the treatment of type 2 diabetes. *Journal of Biomolecular Structure & Dynamics*, 1–16. https://doi.org/10.1080/07391102.2023.2243336

Trott, O., & Olson, A. J. (2010). AutoDock Vina: Improving the speed and accuracy of docking with a new scoring function, efficient optimization, and multithreading. *Journal of Computational Chemistry*, *31*(2), 455–461. https://doi.org/10.1002/jcc.21334

Tsiklauri, L., An, G., Ruszaj, D. M., Alaniya, M., Kemertelidze, E., & Morris, M. E. (2011). Simultaneous determination of the flavonoids robinin and kaempferol in human breast cancer cells by liquid chromatography-tandem mass spectrometry. *Journal of Pharmaceutical and Biomedical Analysis*, *55*(1), 109–113. https://doi.org/10.1016/j.jpba.2010.12.021

von Son-de Fernex, E., Alonso-Díaz, M. Á., Valles-de la Mora, B., Mendoza-de Gives, P., González-Cortazar, M., & Zamilpa, A. (2017). Anthelmintic effect of 2H-chromen-2-one isolated from Gliricidia sepium against Cooperia punctata. *Experimental Parasitology*, *178*, 1–6. https://doi.org/10.1016/j.exppara.2017.04.013

Wang, Z.-Y., Yang, T., Wang, K.-K., Liu, D.-F., Ma, X., Wang, N., Liu, H., Sun, A., & Liu, H. (2023). A water-promoted catalytic hydrodecarboxylation of conjugated carboxylic acids under open air conditions at room temperature. *Green Chemistry*, *25*(8), 3040–3045. https://doi.org/10.1039/D3GC00351E

Wangso, H., Laya, A., Leutcha, P. B., Koubala, B. B., Laurent, S., Henoumont, C., & Talla, E. (2022). Antibacterial and antioxidant activities and phytochemical composition of Stereospermum kunthianum root bark. *Natural Product Research*, *36*(22), 5665–5675.

https://doi.org/10.1080/14786419.2021.2019730

Wei, G., Huang, N., Li, M., Guan, F., Chen, L., Liao, Y., Xie, X., Li, Y., Su, Z., Chen, J., & Liu, Y. (2024). Tetrahydroberberine alleviates high-fat diet-induced hyperlipidemia in mice via augmenting lipoprotein assembly-induced clearance of low-density lipoprotein and intermediate-density lipoprotein. *European Journal of Pharmacology*, *968*, 176433. https://doi.org/10.1016/j.ejphar.2024.176433

Wongsa, P., Bhuyar, P., Tongkoom, K., Spreer, W., & Müller, J. (2023). Influence of hot-air drying methods on the phenolic compounds/allicin content, antioxidant activity and α-amylase/α-glucosidase inhibition of garlic (Allium sativum L.). *European Food Research and Technology*, *249*(2), 523–535. https://doi.org/10.1007/s00217-022-04150-4

Xia, E., He, X., Li, H., Wu, S., Li, S., & Deng, G. (2014). Biological Activities of Polyphenols from Grapes. *Polyphenols in Human Health and Disease*, *1*, 47–58. https://doi.org/10.1016/B978-0-12-398456-2.00005-0

Xiong, Y. L. (2010). Antioxidant Peptides. In *Bioactive Proteins and Peptides as Functional Foods and Nutraceuticals* (pp. 29–42). Wiley-Blackwell. https://doi.org/10.1002/9780813811048.ch3

Yutharaksanukul, P., Tangpromphan, P., Tunsagool, P., Sae-tan, S., Nitisinprasert, S., Somnuk, S., Nakphaichit, M., Pusuntisumpun, N., & Wanikorn, B. (2024). Effects of Purified Vitexin and Iso-Vitexin from Mung Bean Seed Coat on Antihyperglycemic Activity and Gut Microbiota in Overweight Individuals' Modulation. *Nutrients*, *16*(17), 3017. https://doi.org/10.3390/nu16173017

Zehra, A., Nisha, R., Kumar, A., Nandan, D., Ahmad, I., Mahapatra, D. K., Patel, H., Maity, B., & Kumar, P. (2024). Computational Approaches Molecular Docking and MD Simulation Establishes the Potential COVID-19 Main Protease Inhibitors from Natural Products. *Current Chinese Science*, *4*(2), 114–134. https://doi.org/10.2174/0122102981273400231220112631

Zongo, E., Busuioc, A., Meda, R. N.-T., Botezatu, A. V., Mihaila, M. D., Mocanu, A.-M., Avramescu, S. M., Koama, B. K., Kam, S. E., Belem, H., Somda, F. L. S., Ouedraogo, C., Ouedraogo, G. A., & Dinica, R. M. (2023). Exploration of the Antioxidant and Anti-inflammatory Potential of Cassia sieberiana DC and Piliostigma thonningii (Schumach.) Milne-Redh, Traditionally Used in the Treatment of Hepatitis in the Hauts-Bassins Region of Burkina Faso. *Pharmaceuticals*, *16*(1), 133. https://doi.org/10.3390/ph16010133

Declaration of Competing Interest
The authors declare they have no conflict of interest

Graphical abstract

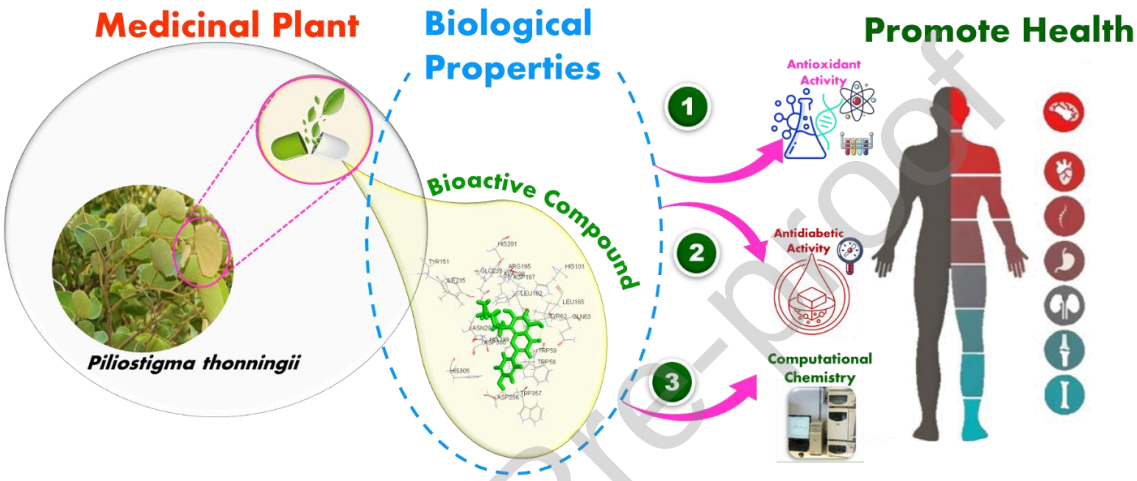

Highlights

- *Piliostigma thonningii* methanolic extract exhibits significant antioxidant activity comparable to synthetic antioxidant BHT.
- Vitexin is identified as a potent natural inhibitor of α-amylase and α-glucosidase, key enzymes in carbohydrate digestion.
- Kaempferol 3-O-α-L-rhamnopyranosyl-(1-2)-β-D-galactopyranoside shows high DPPH anti-radical activity.
- Compounds derived from *P. thonningii* show potential as therapeutic agents for managing type 2 diabetes mellitus.
- *P. thonningii* is an invaluable source of natural antioxidants and anti-diabetic compounds, confirming its traditional medicinal uses.